Chapter 2

Synthesis and characterization of poly (EMA-co-HEMA) copolymeric nanoparticles for encapsulation and in-vitro release of model drug "lamotrigine"

Contents

2.1 Introduction

In recent years, ***nanomaterials***, which exhibit novel properties due to their small size, size quantization and large surface area[1], have attracted so much attention that, a word ''nanomania'', defined as an intense interest in and excitement over the study and application of such materials, has been coined. Nanomaterials are undoubtedly the most prospective new materials of the 21st century. Polymeric nanomaterials have been widely used in the field of information technology, biomedical sciences, catalysis and high performance structural materials. Molecular assembly[2], template chemistry[3], dendrimer polymerization[4], mechanical pulverization[5] and emulsion and microemulsion polymerization[6] are the common approaches used in the preparation of such nanopolymers.

After the appearance of Schulman's introductory articles[7, 8], a series of papers published by Stoffer and Bone[9,10] on oil-in-water microemulsion of methyl methacrylate with SDS as an anionic surfactant and pentanol as cosurfactant for the preparation of monodispersed polymeric nanoparticles of below 50 nm size. Atik and Thomas[11] soon reported the first microemulsion polymerization of styrene using cetyltrimethylammnium bromide as cationic surfactant and 1-hexanol as cosurfactant. They synthesized 20-40 nm sized polystyrene latexes and since then, microemulsion polymerization is attracting researchers in academia and industry[12-30], due to their kinetic and thermodynamic stability, smaller particle size and higher surface area attained only by changing the molar fractions of the components and not the chemical composition. Recently, polymeric microemulsions have been gradually extended to biotechnology[31], catalyzed polymerization[32], immobilization of enzymes[33], novel drug delivery systems[21] and membrane technology[34]. However, microemulsion polymerization presents lots of challenges, such as how to decrease surfactant or cosurfactant concentration, how to increase monomer content and how to improve the purity of final products. Therefore, feasible and effective techniques for microemulsion polymerization are in great demand, and many approaches such as taking advantages of high efficiency surfactants, seed microemulsion polymerization and semi continuous polymerization technique have been developed [35].

Copolymers based on 2-hydroxy ethylmethacrylate have found wide applications in contact lenses, surgery and clinical medicine because of their ability to form biocompatible hydrogels with excellent tolerance and good stability[36-41]. Copolymerization of 2-hydroxy ethyl methacrylate with alkyl acrylate may be of practical interest considering that linear and cross linked copolymers based on 2-hydroxy ethyl methacrylate are widely utilized in ophthalmic industry, as a controlled drug release matrix and as non-thrombogenic materials and surgical prostheses [42-45], etc. Various coworkers [46-48] have reported the controlled polymerization of poly (2-hydroxy ethyl methacrylate) and recently the copolymerization of 2-hydroxy ethyl methacrylate with methacrylic monomers has also been well reported [49-51]. Amongst other applications, these copolymers have been identified as having potential for use in controlled release drug delivery systems[52-54]. In these controlled release systems, the drug is immersed within the core of the glassy polymer, and, as body fluids migrate into the polymer, plasticizing it, the trapped drug is allowed to diffuse through the swollen polymer matrix. Thus, the rate of diffusion of water into the polymer controls the rate of release of the drug, and is dependent on the copolymer composition and microstructure.

In this chapter, we have tried to focus on the copolymerization of ethyl methacrylate, a hydrophobic monomer and hydroxyl ethylmethacrylate, a hydrophilic monomer using redox initiator pair in oil-in-water microemulsion polymerization technique at nearly room temperature. Attempts are made to calculate the reactivity ratio by using linear and non linear least square methods. Lamotrigine as a model antiepileptic drug was selected for entrapment and successive in-vitro release of it from synthesized nanoparticles.

2.2 Experimental

2.2.1 Materials

Drug: Lamotrigine was obtained as a gift sample from Alembic Chemicals Limited, Vadodara, India. Lamotrigine (LAMICTAL) is an antiepileptic drug of the phenyltriazine class. Its chemical name is 3, 5-diamino-6-(2', 3'-dichlorophenyl)-1, 2, 4 -triazine, molecular formula is $C_9H_7N_5Cl_2$, and molecular weight is 256.09. Lamotrigine is a white to pale cream-colored powder and has a pK_a of 5.7.

Lamotrigine is sparingly soluble in water (0.17 mg/mL at 25°C) and slightly soluble in 0.1 M HCl (4.1 mg/mL at 25 °C).

Monomers: Ethyl methacrylate (EMA, Fluka, Buchs, Switzerland), was purified by vacuum distillation under reduced pressure and stored at 4 °C till further use. Hydroxyethyl methacrylate (99%, HEMA, Aldrich, Deutschland, Germany) was used as received.

Initiators & surfactants: L-ascorbic acid (AA) (10% w/v), hydrogen peroxide (HP) (30% w/v), from Merck, Mumbai, India and sodium dodecyl sulphate (SDS) from SD Fine Chem., Baroda, India were used as received.

Solvents and Inhibitors: AR grade methanol, acetone, hexane, tetrahydrofuran and hydroquinone from Merck, India were used as received.

Double distilled deionised water (0.22 micron nylon filtered) was used throughout the experiments.

2.2.2 Preparation of poly (EMA-co-HEMA) copolymeric nanoparticles

The single-phase microemulsion region at 30 and 70 °C was determined visually by titrating aqueous micellar solutions of SDS with monomer mixtures. Copolymeric nanoparticles of various compositions comprising EMA-HEMA monomer mixture (6 % w/w) with monomer weight ratios varying from 90:10 to 50:50 EMA:HEMA, SDS (2 % w/w) and water (92 % w/w) were taken in a three-neck reaction vessel equipped with a nitrogen inlet, thermometer, water condenser and magnetic stirrer. The reaction mixture was stirred at 400 rpm with continuous nitrogen purging for a period of 15 minutes. The reaction temperature was maintained at 40 ± 2 °C and reaction was carried out for 4 h. Appearance of bluish transparent stable latex confirmed the formation of nanoparticles. The polymerization was terminated using hydroquinone as a free radical inhibitor.

- **Separation and purification of nanoparticles**

Most latex requires thorough cleaning following their synthesis in order to ensure the complete removal of potential residues such as monomers, surfactants and solution-borne and surface adsorbed oligomers. For separation and purification of the latexes obtained, reaction mixture was allowed to cool below Kraft temperature of surfactant (i.e. = 16 °C) for the precipitation of surfactant. The precipitated surfactant was removed by filtration and the same procedure was repeated till no further precipitation of surfactant was observed. Copolymeric nanoparticles from any adsorbed surfactant were separated either by lyophilization (Heato Dry winner, Germany) of latex for a period of 24 h or by precipitating latex in 6-8 fold excess volume of methanol: water (70:30) mixture. The adsorbed surfactant was further removed by washing the precipitate with hot water and methanol. Copolymer was further purified by reprecipitating from tetrahydrofuran using methanol to remove traces of unreacted monomers and homopolymer.

2.2.3 Preparation of lamotrigine loaded poly (EMA-co-HEMA) copolymeric nanoparticles

Lamotrigine loaded copolymeric nanoparticles of various compositions were prepared by oil-in-water emulsion polymerization technique[55]. The ternary emulsions comprising EMA and HEMA monomer mixture (6 % w/w) containing 1 % w/w lamotrigine, 2 % w/w SDS and 91 % w/w water were taken in a three-neck reaction vessel equipped with a nitrogen inlet, thermometer, water condenser and magnetic stirrer. Polymerization was initiated at 40 ± 2 °C using redox initiator pair, hydrogen peroxide and L-ascorbic acid, for four hours in order to achieve complete conversion as described earlier. The latex obtained was purified at Kraft temperature of surfactant to achieve surfactant free latex and then it was lyophilized (Heato Dry winner, Germany) to separate nanoparticles as described earlier. The adsorbed surfactant and lamotrigine on the surface of nanoparticles were removed by redispersing lyophilized nanoparticles containing drug in (30:70) water: methanol mixture and centrifuging the suspension at 10,000 rpm for 10 minutes at 16 °C. The supernatant solution was discarded and the procedure was repeated two times. After centrifugation, the centrifuged product was relyophilized for a period of 24 h in order to obtain dry nanoparticles, which were used for further studies.

2.2.4 Characterization techniques

2.2.4.a Fourier transform infrared spectrometry (FTIR)

The Infrared (IR) spectra of purified copolymeric nanoparticles, lamotrigine loaded copolymeric nanoparticles and lamotrigine were recorded on a Perkin Elmer Rx_1 IR spectrophotometer (Massachusetts, USA) using 1-cm diameter KBr pellets.

2.2.4.b Nuclear magnetic resonance spectrometry (NMR)

^1H NMR spectra of poly (ethyl methacrylate) and poly (EMA-co-HEMA) were recorded using 400 MHz ^1H NMR spectrometer (Bruker Specrospin Advance Ultra-shield, Germany) at room temperature (~30 ± 2 °C). The spectra were obtained after accumulating 16 scans by using 1 % sample in $CDCl_3$.

2.2.4.c Gel permeation chromatography (GPC)

Number average ($\overline{Mn}$) and weight average ($\overline{Mw}$) molecular weights of copolymers with different compositions were determined by using Perkin Elmer Totalchrom Gel Permeation Chromatography instrument equipped with turbosec size exclusion software, PE-series 200 RI detector, series 200 isocratic pump and rheodyne injector. The mixed column PLGel 5μ, suitable for molecular weights up to 10^4-10^7 in polar solvent was used and distilled, degassed THF (Merck, India, HPLC Grade) at flow rate of 1 ml/min was used as an eluent. Medium molecular weight polystyrene standards (POLYSCI, 1 mg/mL in THF, with molecular weight $1\text{x}10^3$-$3\text{x}10^5$) were used for calibration of GPC.

2.2.4.d Dynamic light scattering (DLS)

A Brookhaven's 90 plus dynamic light scattering equipment (Holtsville, USA) with a 15 mW solid state laser source operated at 688 nm was used to measure the particle size and size distribution of the polymerized latex in a dynamic mode. For light scattering measurements, in order to minimize the inter particle interactions, the analysis of the latex was done after 10 times dilution considering the refractive index and viscosity of water as that of latex. The particle size was obtained from the Stokes-Einstein relation

$$\boxed{D = KT / (3 \pi \eta d)} \qquad (1)$$

Where d is the diameter of particles, D is translational diffusion coefficient, K is Boltzmann constant, T is temperature (^{o}C) and η is the viscosity of the medium (centi poises). The scattering intensities from the samples were measured at 90^{o} using photomultiplier tube. All the measurements were performed in triplicate.

2.2.4.e Transmission electron microscopy (TEM)

TEM analysis of placebo nanoparticles and drug loaded copolymeric nanoparticles was performed using JEOL 1200 EX Transmission Electron Microscope at accelerating voltage of 80 KeV. One drop of polymeric latex was dispersed in 5 mL of water and was placed on the 200 mesh carbon coated copper grid. The grid was dried under IR lamp for a period of 10 minutes and then the images of representative areas were captured at suitable magnifications.

2.2.4.f Estimation of percentage encapsulation efficiency

The UV spectrum of the purified copolymeric nanoparticles, lamotrigine and lamotrigine loaded copolymeric nanoparticles were recorded on a Perkin Elmer Lambda 35 UV/Vis spectrophotometer. Ten milligrams of purified nanoparticles containing drug were dissolved in ten mL of absolute alcohol. Entrapment efficiency (% EE) of lamotrigine in nanoparticles was calculated from the calibration plot constructed at 306 nm after confirming the noninterference of polymers in the absorption region of lamotrigine.

2.2.4.g Swelling study

The swelling study of the lamotrigine loaded copolymeric nanoparticles was done in the simulated gastric environment with 0.1M HCl. The Swelling of copolymeric nanoparticles was measured by equilibrium weight gain method[56] up to 15 h till an equilibrium is attained in an incubator (Stuart Orbital Incubator, Model S150, Staffordshire, UK) maintained at 37 ± 2 °C. Liquid droplets adhered on the surface of the particles were removed using tissue paper and the swollen particles were weighed on an electronic balance (Mettler, Model AE 240, Griefensee, Switzerland) with an accuracy of ± 0.1 mg. The nanoparticles were dried in an oven at

60 °C for 5 h until there was no change in the dry weight of the samples. From the dry weight W_1 and equilibrium weight W_2 of the sample, water uptake Q was calculated by using equation (2):

$$\boxed{Q=\left(\frac{Weight\ of\ swollen\ particles\ (W_2)-Weight\ of\ dry\ particles\ (W_1)}{Weight\ of\ dry\ particles\ (W_1)}\right)\times 100} \qquad (2)$$

2.2.4.h In-vitro release

In-vitro release study for drug loaded polymeric nanoparticles of various compositions was carried out in a dialysis bag (cut-off 10,000, Hi-Media, India) diffusion technique[57]. Drug release from the nanoparticles was studied in 0.1M HCl, which is according to FDA is a dissolution medium for lamotrigine. The aqueous nanoparticulate dispersion equivalent to 1 mg lamotrigine was placed in cellulose dialysis bag, sealed at both ends. The dialysis bag was immersed in the receptor compartment containing 50 mL of the dissolution medium, and stirred at 100 rpm under magnetic stirring. Aliquots of samples were withdrawn at regular time intervals and the same volume was replaced with fresh dissolution medium. The samples were analyzed by UV spectrophotometer at 306 nm against blank. All experiments were repeated thrice and the average values were considered. Drug release kinetics study was also performed with the help of different mathematical models available.

2.2.4.i Stability studies

Short term stability study was carried out for all batches. The formulations were stored in air tight sealed vials at 2-8 °C and 30 ± 2 °C. The preparations were sampled at regular intervals of 0, 10, 20 and 30 days and tested for the particle size and % drug retained. Lyophilized powder was vortexed with aliquots (2 mL) of the distilled water and subjected to centrifugation on a laboratory centrifuge (Remi C24, Mumbai, India) at 5000 rpm. The clear supernatant was siphoned off carefully to separate out free lamotrigine if any, from nanoparticles on storage. Absolute alcohol (2 mL) was added to the supernatant to lyses the nanoparticles and the absorbance was recorded at 306 nm.

2.3 Results and Discussion

In the present study, attempts are made to prepare copolymeric Nanoparticles of ethylmethacrylate and 2-hydroxyethyl methacrylate in microemulsions containing anionic surfactant SDS. Prior to polymerization the reaction mixture was translucent at the reaction temperature (40 ± 2 °C) and as polymerization proceeded, the mixtures developed a bluish tint, indicating the formation of polymeric nanoparticles. The microlatex, especially the o/w, requires high surfactant concentration to form stable polymer latex with high polymer content. Latex with low polymer content or with high surfactant concentration limits the industrial applications. Hence it is desirable to minimize the surfactant amount and maximize the polymer content.

In this study hydrophilic monomer HEMA was used as reactive cosurfactant to minimize surfactant concentration. When the reactive cosurfactant is added to the latex, it copolymerizes with the monomer and forms latex particles. Effect of EMA: HEMA concentration ratio on properties of the copolymeric Nanoparticles and on entrapment and release studies of lamotrigine is undertaken. Copolymeric Nanoparticles were prepared, separated and purified as described in section 2.2.2 and 2.2.3 and were used for further studies.

2.3.1 Fourier transform infrared spectrometry (FTIR)

FTIR spectra of lamotrigine loaded copolymeric nanoparticles, placebo copolymeric nanoparticles and free lamotrigine were recorded and are given in ***Figure 2.1.*** As seen in ***Figure 2.1A***, the characteristic bands of lamotrigine appeared at 3451, 1620, 1500-1350, 800 and 550 cm^{-1}, due to presence of stretching and bending vibrations of -NH_2 groups, ring stretching vibration due to -C=C and -C≡N bonds, m-substituted ring vibration and presence of C-Cl bond in lamotrigine. While for copolymeric nanoparticles ***(Figure 2.1B)***, the appearance of the broad band at 3500 cm^{-1} is due to -OH stretching vibrations of HEMA unit and bands at 1728 cm^{-1} for >C=O stretching due to both EMA and HEMA units confirmed the copolymer formation. The bands at 2852, 2923, 1482 and 1389 cm^{-1} are attributed to stretching and bending vibrations of -CH_2, >CH groups of EMA and HEMA unit of copolymer. Bands appearing at 1045 cm^{-1} and 1245 cm^{-1} correspond to ester group from EMA and HEMA units of copolymer. But in the case of drug loaded copolymeric nanoparticles ***(Figure 2.1C),*** it was observed that the broad hydroxyl band of copolymer is partially replaced superimposed by sharp band due to N-H stretching at 3451 cm^{-1} and an additional new band appears at 1620 cm^{-1} corresponding to N-H bending vibration. Appearance of ring stretching bands due to -C=C and -C≡N bonds of lamotrigine around 1300-1500 cm^{-1} confirmed the drug entrapment in the polymeric matrix.

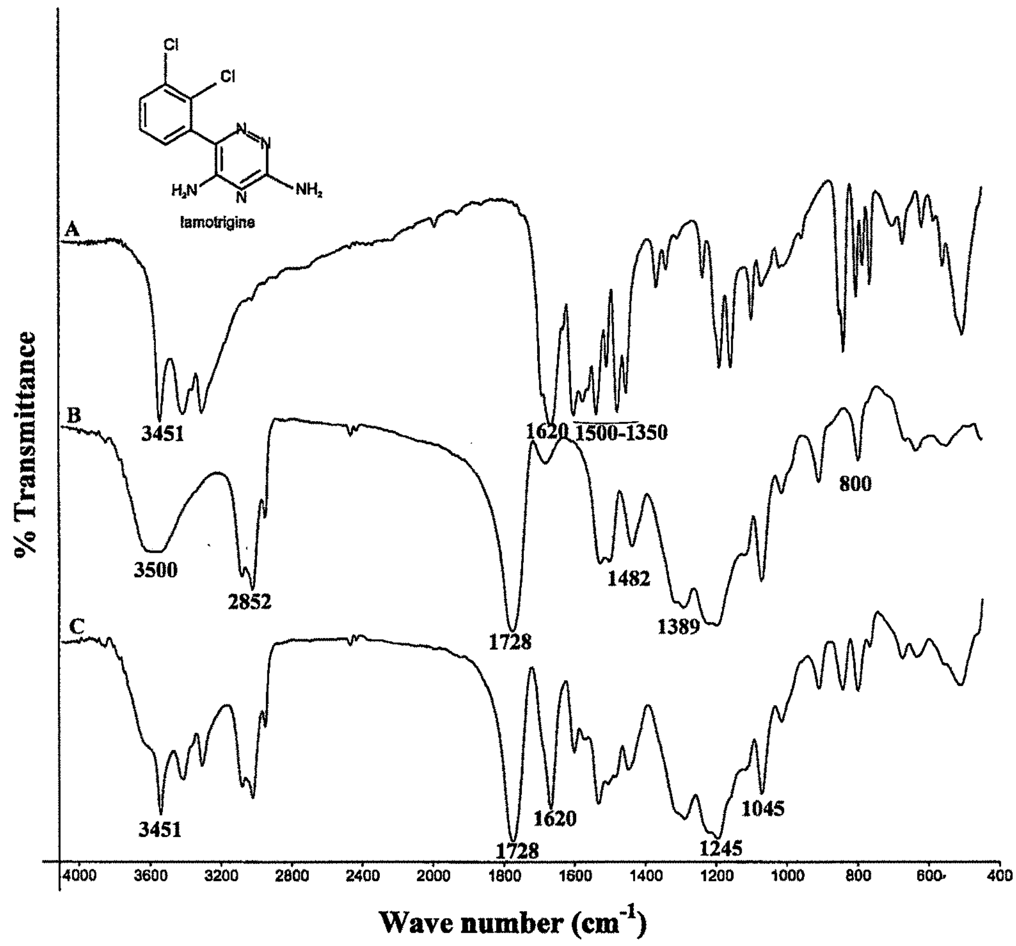

Figure 2.1 FTIR spectra of (A) lamotrigine (B) copolymeric nanoparticles and (C) lamotrigine loaded copolymeric nanoparticles.

2.3.2 Determination of reactivity ratio

In any copolymerization reaction, the reactivity and the relative concentrations of the two monomers determine the concentration of each comonomer that is incorporated into the copolymer and also influence the sequencing of monomers. The chemical structures of these monomers strongly influence reactivity during copolymerization. Copolymers with unlimited number of different sequential arrangements can be produced just by changing relative amounts and chemical structures of the monomers or changing the experimental conditions. As a result materials of varying chemical and physical properties are produced. Different types of copolymers such as random, alternative, graft and block can be synthesized by modulating the processing conditions.

Hill *et al*[58] recently reported the copolymerization of HEMA with cyclohexyl methacrylate (CHMA) and butyl methacrylate (BMA) by bulk polymerization. They reported the values of $r_{HEMA} = 1.73$ and $r_{BMA} = 0.65$ for HEMA-BMA pair and $r_{HEMA} = 1.26$ and $r_{CMA} = 0.31$ for HEMA-CMA monomer pair.

Barson and coworkers[59-62] and Verma and Patnaik[63] have reported the effect of temperature on the monomer reactivity ratios for copolymerization of styrene and cinnamic acid and its esters and hydroxyethylmethacrylate with alkyl acrylates respectively. They have reported that size of the substituents in the acrylic acid esters influences the reactivity ratio e.g. the substitution of alpha hydrogen with methyl group increase the relative reactivity of the alkyl acrylate monomers towards HEMA.

Fernandez-Garcia *et al*[64] and Ito *et al*[65] have reported the effect of solvent polarity on the reactivity of HEMA. HEMA being an amphiphilic monomer exhibits different polymerization behavior in different solvents. They have reported that in copolymerization of BMA with HEMA in dimethyl formamide (DMF), reactivity ratio were observed to be $r_{BMA} = 0.84$ and $r_{HEMA}= 0.98$[64]. While in the copolymerization of hydroxyl ethylmethacrylate - lauryl methacrylate monomer pair (HEMA-LMA) in benzene, the reactivity of HEMA was observed to be as high as 11.2 due to low dipole moment of benzene and in DMF the reactivity of HEMA was observed to be 0.8. The difference was attributed to the difference in tendency of HEMA to form aggregates in two solvents[65].

Reactivity of monomer also depends on the microenvironment of polymerization. Gan *et al*[66] and Xu *et al*[67] have attributed the observed difference in the reactivity's in bulk and microemulsion medium of styrene and methyl methacrylate monomer pair. The results were discussed in terms of the partitioning of monomers in the microemulsions and the copolymerization loci.

Sanghavi *et al*[68] discussed elaborately the effect of partially water soluble monomer and completely water soluble monomer pair (STY/AN and STY/HEMA) on their reactivity ratio in emulsion and microemulsion copolymerization by considering actual concentration variation at polymerization loci due to partitioning of the monomer, and examined the sequence distribution in copolymer theoretically and by ^{13}C NMR analysis.

The amount of the comonomer that has been incorporated into the copolymer is determined through various analytical methods such as ^{1}H NMR, ^{13}C NMR, FTIR, UV-Visible and Raman spectrometry.

In 1997 Polic *et al*[69] have presented a comprehensive literature survey regarding estimation of reactivity ratios. ***Table 2.1*** gives summary of works done in last 10 years on estimation of reactivity ratios by linear and non linear least square methods for different monomer pairs. ***Table 2.2*** gives abbreviations used in ***Table 2.1***.

Table 2.1 Summary of work on reactivity ratios estimated through different methods.

Ref.	Author	Method	Systems	Year
70	Abdollahi M and Sharifpour	NLLS	VA/MA, online ^{1}H NMR kinetic experiment at 60 ^{0}C in benzene	2007
71	Aguilar et al	NLLS	HEMA/AMPS, DMAA/AMPS	2002
72	Belleney et al	FR,KT,TM	MMA,PMEM,PEEM/MA; MMA/PMEM/MA	2002
73	Bernhardt et al	NLO	Methylated β-cyclodextrin with hydrophobic acrylates	2001
74	Bhawal et al	FR, NLLS	Recalculation of monomer reactivity for MMA/EA, STY/MA monomer pair in emulsion and microemulsion media.	2002
75	Bhawal et al	FR, NLLS	STY/MA, STY/MMA; and STY/AN system; considering the effect of monomer partitioning in microemulsion media.	2002

76	Brar and Dutta	KT	AN/ Hexyl methacrylate	1998
77	Brar and Hekmatyar	KT,EVM	AN/STY/MMA	1999
78	Brar and Yadav	KT,EVM	GMA/Vinylidene chloride	2003
79	Brar et al	KT,EVM	N-vinyl carbazole / BMA	2003
80	Brar et al	KT, EVM	HEMA/ MA, Bulk Polym.	2007
81	Buback and Wittkowski	NLO	Ethene with AA and MAA	2000
82	Camail et al	ML	acrylamide, acrylic acid and N-(1,1-dimethyl-3-oxobutyl)acrylamide;	1998
83	Catalgil-Giz et al	EVM	STY/MMA; on-line monitoring	2002
84	Chambard et al	NLLS	Sty/BA	1999
85,86	Coskun et al	KT,FR, ML	3-phthalimido-2-HPMA/STY	2002

87	Czerwinski	KT, NLLS	STY/methyl α-cyanocinnamate	1997a,1998b
88	De and Sathyanarayana	NLO	Indene/alkyl acrylates; Tg information	2002
89		NLO	Indene/p-tert-butylstyrene; thermal degradation; Tg studies	2002
90		FR,KT	MMA/VAc/Molecular Oxygen	2002
91	Demirelli et al	FR,KT	(3-mesityl-3-methylcyclobutyl)-2-HEMA with AN	2000
92	Dubois et al	FR, KT, NLLS	MMA/Functionalized Methacrylate	2005
93	Erbil et al	TM	Itaconic acid/ acrylamide	2000
94	Erol and Soykan	FR,KT	MMA/2-methylbenzyl methacrylate and 4-methylbenzyl methacrylate	2002

95	Fernandez-Garcia et al	NLLS	2-HEMA/BMA	2000
96		TM	2-HEMA/ STY, STY/BA	1999
97	Galimberti et al	NLO	Ethene/propene; use of C13-NMR data	1998
98		NLO	Ethene/propene with metallocenes	1999
99	Habibi et al	GLS	lauryl methacrylate–isobutyl methacrylate in bulk	2003
100	Haddleton et al	NLO	MMA and BMA in anionic radical and living radical polymerizations	1997
101	Hakim et al	EVM,NLLS	BA/MMA; solution polymerization	2000
102	Hill et al	NLLS	HEMA/BMA, HEMA/CMA, bulk polymerization	2000
103	Ito et al	KT	Hydroxystyrene derivatives with t-BMA	2000

			and t-BA	
104	Kaim et al	NLO	STY/AN; solvent effect	2000
105		NLO	STY/MMA; solvent effect	1999
106		Simplex algorithm	STY/MMA; bulk	1999
107		Simplex algorithm	STY/AN terminal and penultimate model; solvent effect	1998
108	Kucharski and Lubczak	KT, FR	Hydroxyalkyl methacrylates with acryl- - amide and methacrylamide	1997
109	Manders et al	TM	MMA/BMA	1997
110	Madruga et al	NLLS	HEMA/t-BA, Solution Polymerization	2000
111	McManus et al	EVM	AMS/BA; bulk	2002
112			AN/VAc; bulk	1998

113			STY/HEA; STY/HEA/EA	1998
114	Monett et al	FR,KT,TM, GA	MMA/MVE	2002
115	Palmer et al	EVM	AMS/MMA	2001
116	Palmer et al	EVM	AMS/MMA	2000
117	Rainaldi et al	KT	AA/HEMA; template polymerization	2000
118	Roos et al	NLO	BA/MMA	1999
119	Ryttel	FR,KT	EMA with halophenyl maleimides	1999
120	Sanghvi et al	FR, KT,TM	STY /AN; microemulsion	2000
68	Sanghvi et al	FR, KT,TM, NLLS	STY/HEMA; microemulsion	2002
121	Scorah et al	EVM	MMA/VAc; bulk/solution; low conversions	2001
122	Senthilkumar et al	FR,KT	Phthalimido EMA/GMA	2001

123	Stergiou et al	FR,KT	STY/alkyl methacrylates; thermal properties	2002
124	Thamizharasi et al	FR,KT,EKT	MMA and BA with acetylphenyl acrylate	1997
125		FR,KT,EKT	GMA with 4-nitrophenyl acrylate	1997
126		FR,KT,EKT	4-Nitrophenyl acrylate/MMA	1999
127		FR,KT,EKT	MA with CPA; applications in leather industry	1999
128	Van Den Brink et al	NLLS	MMA/MBL; on-line Raman Spectrometry	1999
129	Vijayanand et al	KT,FR,EVM	BCPA/MMA; solution; low conversions	2003
130	Vijayanand et al	KT,FR,EVM	DMPMA/MMA; low conversion	2002
131	Zaldivar et al	KT,TM,ML	Acrylic acid/VAc	1997
132	Zhao et al	NLO	STY/n-butyl maleimide	2002

133	Ziaee and Nekoomanesh	FR,KT,EKT, MH	STY/BA	1997

Table 2.2 Abbreviations used in Table 2.1.

* Methods for reactivity ratio determination.

Abbreviation	Description
AA	Acrylic acid
AMS	α-methyl styrene
AN	Acrylonitrile
BA	Butyl acrylate
BMA	Butyl methacrylate
CPA	Chlorophenyl acrylate
DMF	N,N'-dimethylformamide
EA	Ethyl acrylate
EKT*	Extended Kelen-Tudos method
EMA	Ethyl methacrylate
EVM*	Error-in-variables-model
FR*	Fineman-Ross method
GA	Genetic Algorithm
GLS	General Linear Squares
GMA	Glycidyl methacrylate
HEA	Hydroxyethyl acrylate
HEMA	2-hydroxyethyl methacrylate
HPMA	Hydroxypropyl methacrylate
KT*	Kelen-Tudos method
MA	Methyl acrylate
MAA	Methacrylic acid
MH*	Mao-Huglin method
ML*	Mayo-Lewis method
MMA	Methyl methacrylate
NLLS*	Nonlinear least squares method
NLO*	Nonlinear optimization method
STY	Styrene
TM*	Tidwell-Mortimer method

The high resolution ^{1}H NMR spectra of poly (ethyl methacrylate) and poly (EMA-HEMA) copolymer are shown in ***Figure 2.2.*** The composition of the copolymer was evaluated from the relative intensity of $-\underline{CH_2}-O$ of the HEMA and $-O-\underline{CH_2}$ ester group of the methacrylate units using the following relationship.

$$F_s = \frac{2\,I(-O-\underline{CH_2})}{2\,I(-O-\underline{CH_2}) + 5\,I(-\underline{CH_2}-O)} \quad (3)$$

Where I (-O-$\underline{CH_2}$) and I (–$\underline{CH_2}$ –O) represents the total peak area for the protons of -O-$\underline{CH_2}$ and –$\underline{CH_2}$ –O groups of EMA and HEMA respectively. Fs are the mole fractions of ethyl methacrylate in the copolymer and the results obtained are summarized in ***Table 2.3***.

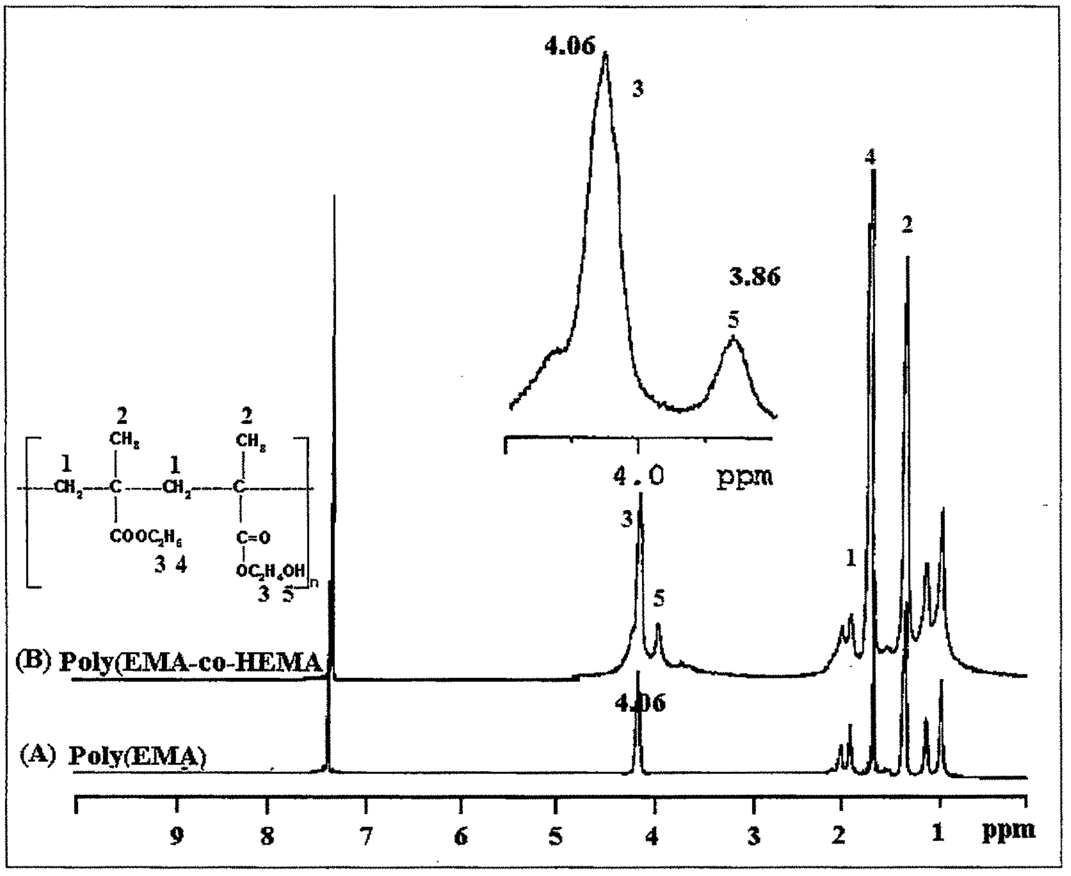

Figure 2.2 Representative ^{1}H NMR spectra of (A) EMA homopolymer and (B) EMA: HEMA (70:30) copolymer.

Table 2.3 Mole fractions of monomers in feed and copolymers.

(EMA:HEMA) mole ratio in feed	Mole fractions in feed		Mole fractions in copolymers from NMR		% Conversion
	M_{EMA}	M_{HEMA}	P_{EMA}	P_{HEMA}	
90:10	0.9	0.1	0.82	0.18	7.1
80:20	0.8	0.2	0.69	0.31	6.4
70:30	0.7	0.3	0.58	0.42	4.3
60:40	0.6	0.4	0.55	0.45	5.9
50:50	0.5	0.5	0.51	0.49	8.3

After calculating the composition, reactivity ratios of EMA-HEMA monomer pair in the microemulsion were determined at less than 10 % conversion by traditional methods like Fineman–Ross[134], Inverted Fineman Ross[134], Kelen-Tudos[135] linear least square methods and most reliable nonlinear least square Tidwell-Mortimer methods [136]. For calculation of reactivity ratios by above methods, parameters needed are listed in ***Table 2.4.***

- ***Fineman-Ross method (FR)***

The FR method is based on the following equation:

$$\boxed{G = \frac{M}{P}(P-1)} \qquad (4)$$

$$\boxed{F = \frac{M^2}{P}} \qquad (5)$$

where M is the ratio of mole fraction of monomer in the feed and P is the ratio of mole fraction of monomer unit in copolymer. The linear relationship between G and F could be given as;

$$\boxed{G = Fr_1 - r_2} \qquad (6)$$

For this method, by plotting G versus F for all experiments, one can obtain a straight line where the slope of the straight line is the value for r_{EMA} and the intercept of the line is the value for r_{HEMA}. A main advantage in determining the reactivity ratio by this method is that, it gives a qualitative observation of the validility of the intersection area. However, the quantitative estimate of error is impossible. Therefore, weighting of the data is needed to determine the most precise values of r_{EMA} and $r_{HEMA,}$ because the high and low experimental composition data are unequally weighted, which produces large effects on the calculated values of r_{EMA} and r_{HEMA}. ***Figure 2.3*** is the linear plot obtained by using the above equation and the necessary calculated parameters are given in ***Table 2.4***. The obtained values of r_{EMA} and r_{HEMA} by this method were ***0.42*** and ***0.58*** respectively. Reactivities can also be calculated through Inverted FR method. Slope and intercept of the best fitted line obtained by using equation 5 gave reactivity's of EMA and HEMA to be ***0.40*** and ***0.54*** respectively ***(Figure 2.4)***.

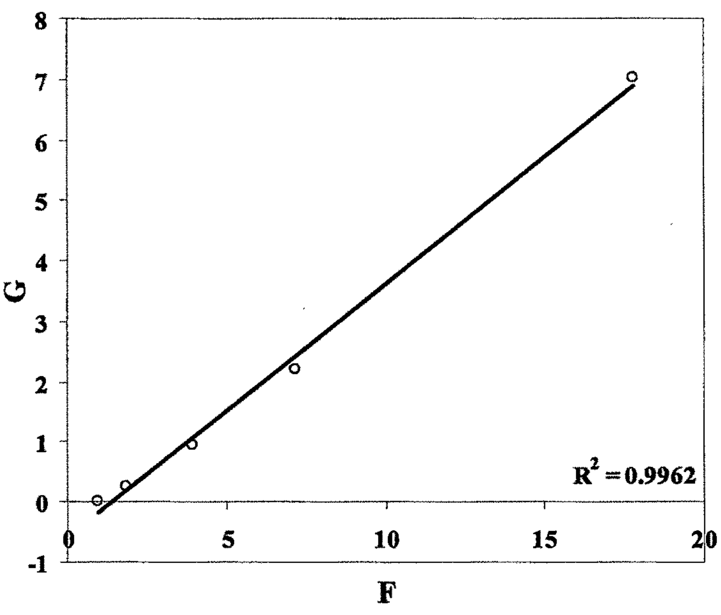

Figure 2.3 Fineman-Ross method.

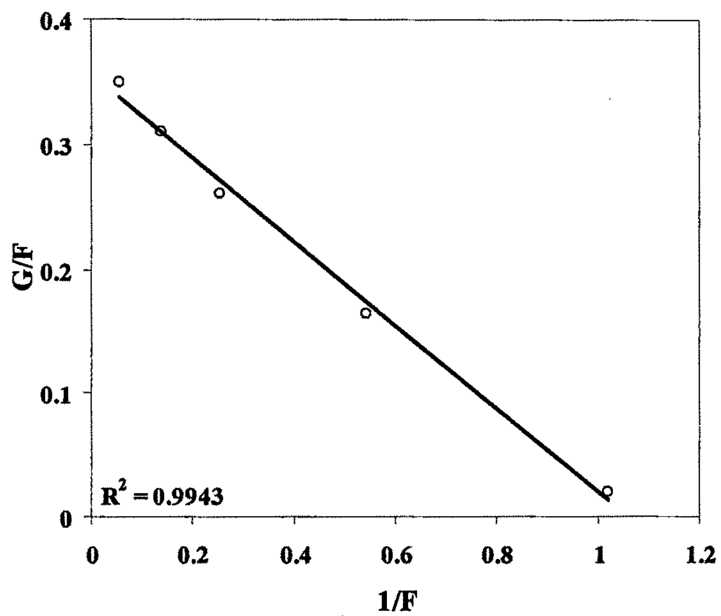

Figure 2.4 Inverted Fineman-Ross method.

- ***Kelan - Tudos***

A refinement of the linearization method was introduced by Kelan-Tudos by adding an arbitrary positive constant α into the Fineman-Ross equation. This technique spreads the data more evenly over the entire composition range to produce equal weighting to all the data. The Kelan-Tudos's refined form of the copolymer equation is as follows:

$$\eta = [r_{EMA} + r_{HEMA}/\alpha]\ \xi - r_{HEMA} / \alpha \tag{7}$$

Where:

$$\eta = G / (\alpha + F) \tag{8}$$

$$\xi = F / (\alpha + F) \tag{9}$$

By plotting η versus ξ, a straight line is produced that gives $-r_{HEMA} / \alpha$ and r_{EMA} as the intercepts, on extrapolation to ξ=0 and ξ=1, respectively. Distribution of the experimental data symmetrically on the plot is performed by choosing the value to be $(F_m F_M)^{1/2}$, where F_m and F_M are the lowest and highest F values, respectively. By this method, the reactivity ratio values obtained for r_{EMA} and r_{HEMA} are ***0.33*** and ***0.82*** ***(Figure 2.5).***

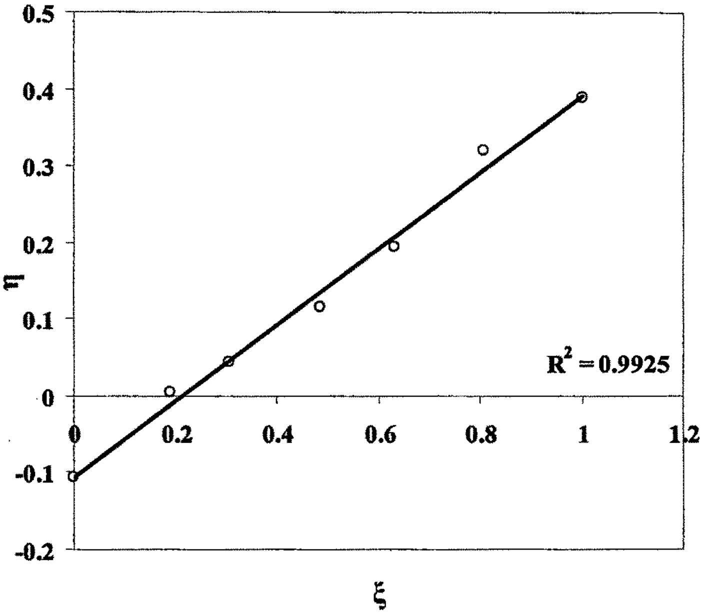

Figure 2.5 Kelan –Tudos method.

- ***Mortimer-Tidwell method***

The main advantage of the above mentioned methods used for the determination of reactivity ratio is that the results can be qualitatively checked and the main disadvantage is a direct dependence of the composition on conversion for most polymer systems and therefore, low conversion is needed to determine the reactivity ratios. Furthermore, extensive calculations are required, but only qualitative measurements of precision can be obtained and precise reactivity ratio determination is hard to reproduce from one experiment to another.

Therefore, a technique that allows the precise application of statistical analysis for r_1 and r_2 was proposed by Tidwell-Mortimer, which they called the non-linear least-square method and is considered to be one of the most accurate procedures for determination of monomer reactivity ratios. This method can be considered to be a modification or extension of curve fitting method, where for selected values of r_1 and r_2, the sum of the squares of the difference between the observed and computed polymer composition is minimized. Using these criteria for the nonlinear least squares method of analysis, the values for the reactivity ratios are unique for a given set of data, where all investigations arrive at the same values for r_1 and r_2. The computer program produces reactivity ratios for the monomer in the system with a 95 % joint confidence limit. The joint confidence limit is a quantitative estimation of the validity of the results of the experiments and calculation performed. This method of data analysis consists of obtaining estimates of the reactivity ratios for the system based on experimental data of monomer in feed and monomer that is incorporated into the copolymer, both in mole fractions. Several iterations were performed in order to determine a pair of reactivity ratios that fit the criteria, wherein the value of the sum of the squares of the differences between the observed and computed polymer composition is minimized. The use of the Gauss-Newton nonlinear least squares procedure predicts the reactivity ratios for a given set of data after repeating the calculations so that the difference between the experimental data points and the calculated data points on a plot of mole fraction of monomer incorporated versus monomer in the feed is reduced to the minimum value. Therefore, the last iteration of the calculations produces a convergence on the least squares estimate of r_1 and r_2. A brief description of the method consists, initial estimates of r_1 and r_2, a set of computations performed yielding the sum of the squares of the differences between the observed and computed polymer compositions. The summation is then minimized by iteration, yielding reactivity ratio. By this method, the reactivity ratio values obtained for r_{EMA} and r_{HEMA} in our study were ***0.36*** and ***0.41 (Figure 2.6)***. It was well reported in the literature that the product of r_1 and r_2 decides the character of the obtained copolymer. Here in this case the product of r_1 and r_2 was observed to be less than 1 indicating the tendency of formation of random copolymer.

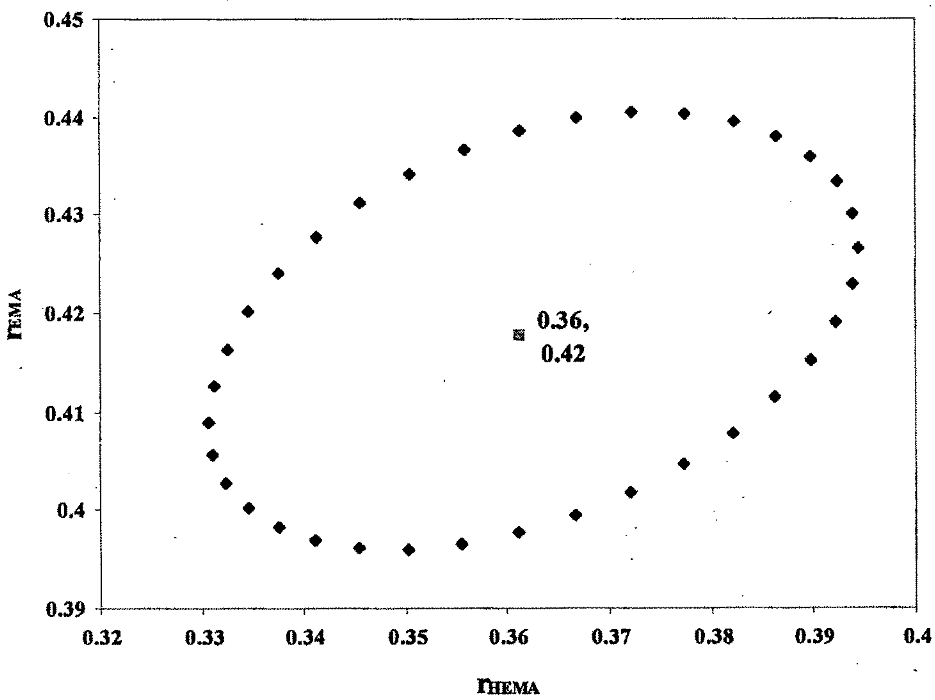

Figure 2.6 Tidwell-Mortimer nonlinear least square method.

Table 2.4 The calculated parameters useful in the determination of reactivity ratios at < 8 % conversion.

M_E	M_H	P_E	P_H	M	P	G	F	G/F	1/F	ά	ά +F	η	ε
0.9	0.1	0.82	0.18	9.0	4.55	7.02	17.80	0.35	0.06	4.18	22.0	0.32	0.81
0.8	0.2	0.69	0.31	4.0	2.23	2.20	7.17	0.31	0.14	4.18	11.4	0.19	0.63
0.7	0.3	0.58	0.42	2.33	1.38	0.94	3.96	0.26	0.25	4.18	8.14	0.12	0.49
0.6	0.4	0.55	0.45	1.50	1.22	0.27	1.84	0.17	0.54	4.18	6.02	0.05	0.31
0.5	0.5	0.51	0.49	1.0	1.02	0.02	0.98	0.02	1.02	4.18	5.16	0.004	0.19

M_E = Mole Fraction of EMA in Feed

M_H = Mole Fraction of HEMA in Feed

P_E = Mole Fraction of EMA in Copolymer

P_H = Mole Fraction of HEMA in Copolymer

M = M_E / M_H

P = P_E / P_H

G = $M (P-1) / P$

F = M^2 / P

ά = $(F_m F_M)^{1/2}$

η = G / ά +F

ε = F / ά +F

2.3.3 Molecular weight determination

The molecular weight of the synthesized copolymers as estimated against polystyrene standard by GPC was in the range of 3.08-2.01 x 10^5 and polydispersity was in the range of 1.1-1.88. It was observed that as the HEMA content increases in the copolymer, the molecular weight of the copolymer decreases and polydispersity increases as observed from ***Figure 2.7***.

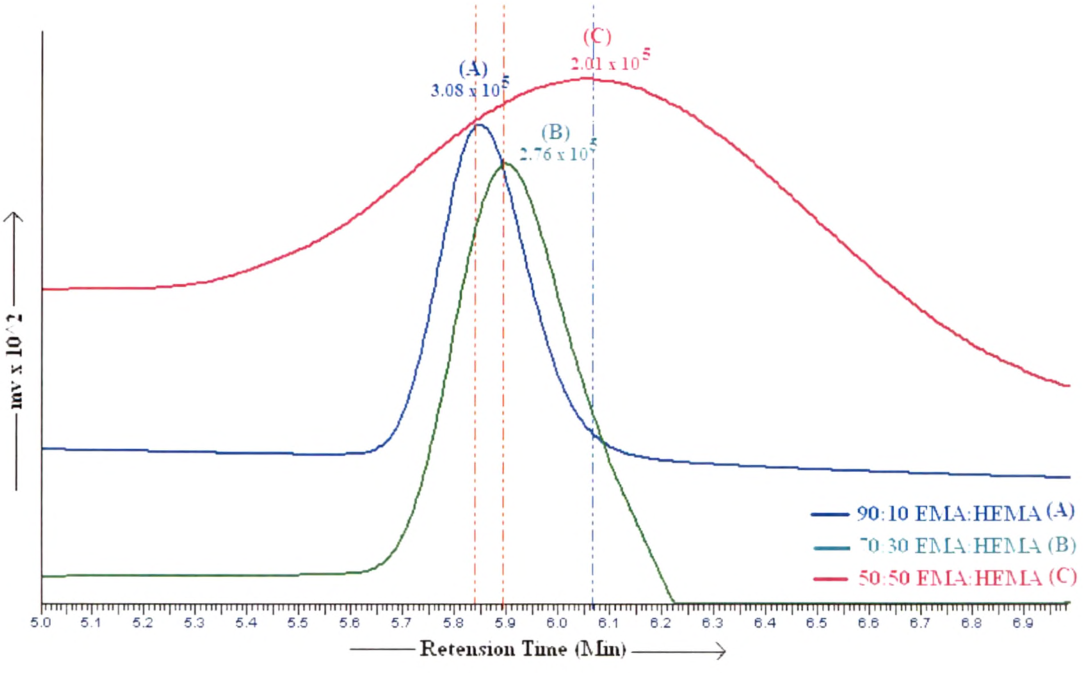

Figure 2.7 Effect of copolymer composition on molecular weight distribution by GPC.

2.3.4 Particle size analysis

Particle size of the lamotrigine loaded copolymeric nanoparticles was determined through dynamic light scattering technique and transmission electron microscopy ***(Figure 2. 8 and 2.9)***. The particle size histograms obtained through DLS for 90:10 to 50:50 (EMA: HEMA) copolymers are given in Figure 2.8. The particle size was observed to be in the range of 30 ± 5 nm for all copolymer compositions and the data is compiled in ***Table 2.5***. Here it was observed from the DLS results that, particle size is independent with respect to copolymer composition.

Transmission electron microscopy (TEM) was used to examine size and morphology of copolymeric nanoparticles. ***Figure 2.9*** shows TEM images of 90:10 ***(2.9A)*** and 50:50 ***(2.9B)*** (EMA: HEMA) placebo copolymeric nanoparticles and ***Figure 2.9 C*** shows the TEM image of lamotrigine loaded copolymeric nanoparticles (90:10). Particle sizes were observed approximately in the range of 20 ± 5 nm diameter with spherical morphology and monodispersed in nature for 90:10 poly (EMA: HEMA) copolymer, but as we increase the HEMA content in the copolymer, some agglomeration was observed in the particles, which is seen from the TEM image of the 50:50 poly (EMA: HEMA) latex. In the case of lamotrigine loaded nanoparticles (90:10 EMA: HEMA), spherical and monodispersed particles are observed and size was observed approximately in the range of 25 ± 5 nm.

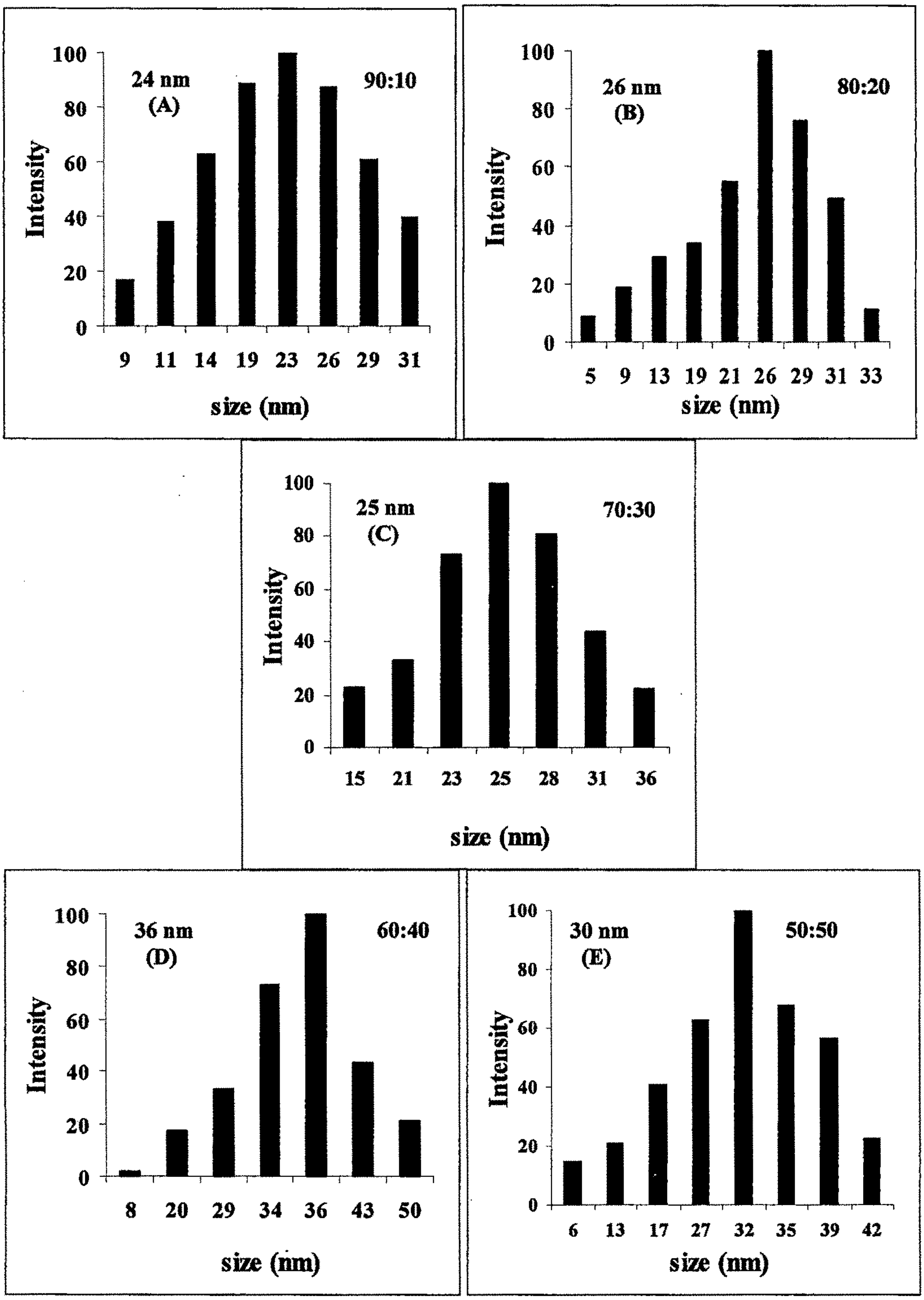

Figure 2.8 **Particle size distribution of poly (EMA: HEMA) copolymeric nanoparticles by dynamic light scattering. (A) 90:10, (B) 80:20, (C) 70:30, (D) 60:40, and (E) 50:50 EMA: HEMA.**

(A) TEM image of 90:10 poly (EMA: HEMA)

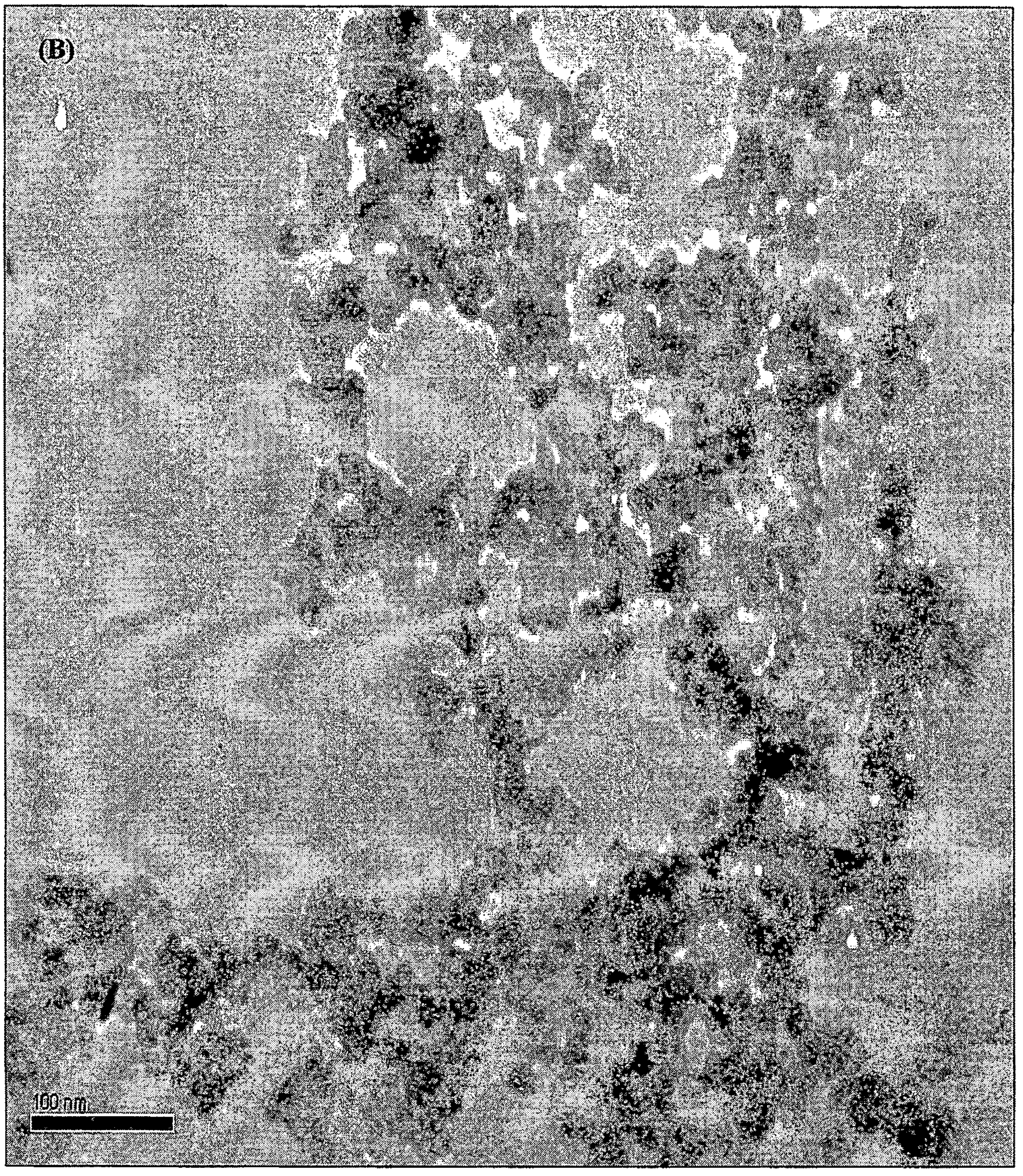

(B) TEM image of 50:50 poly (EMA: HEMA)

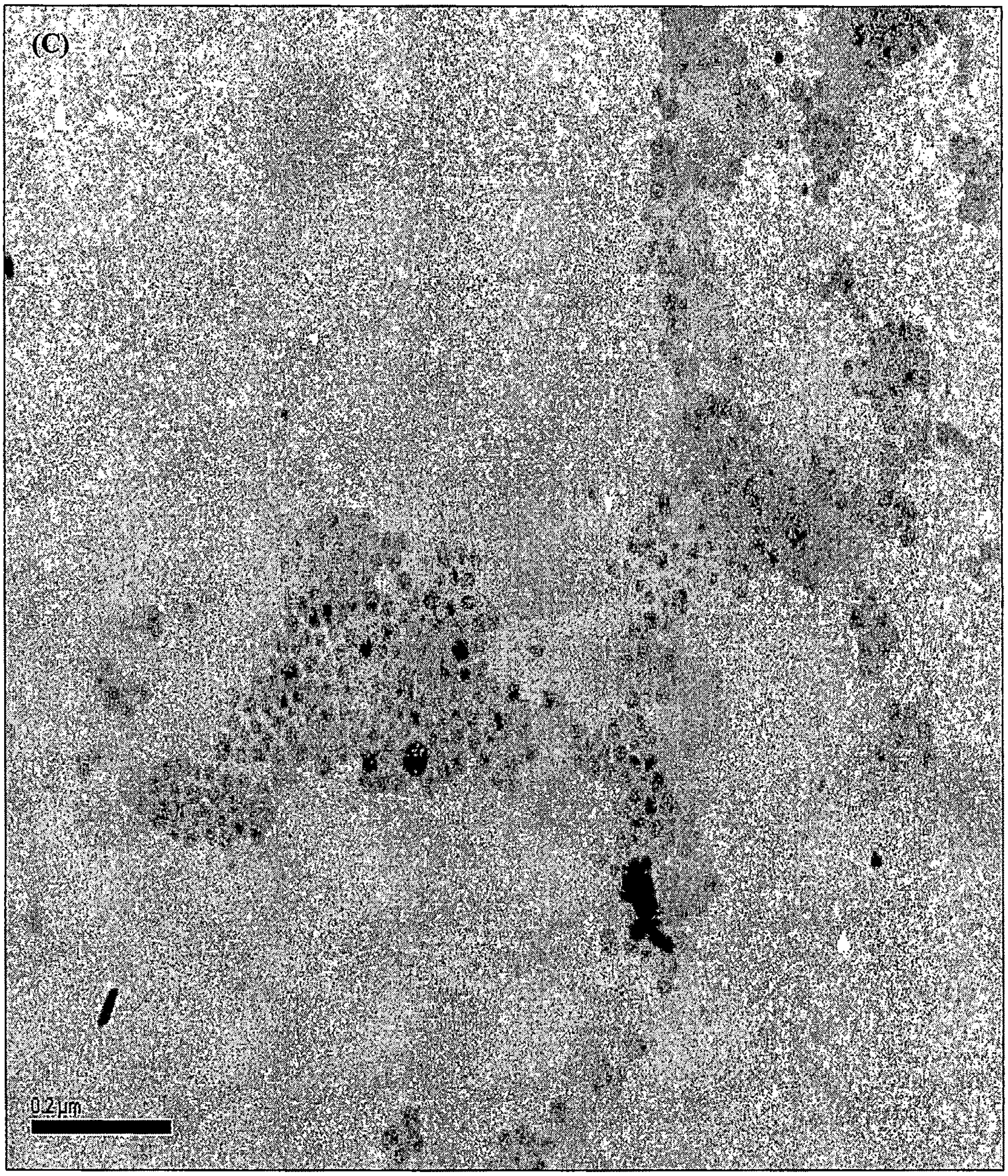

(C) TEM image of 90:10 lamotrigine loaded poly (EMA: HEMA)

Figure 2.9 **TEM images of copolymeric nanoparticles**

(A) 90:10 poly (EMA: HEMA),

(B) 50:50 poly (EMA: HEMA) and

(C) lamotrigine loaded 90:10 poly (EMA: HEMA)

2.3.5 Entrapment efficiency of lamotrigine in nanoparticles

Efficiency of entrapment of lamotrigine in copolymeric nanoparticles was determined by using UV-Visible spectrometry as described in section 2.2.4.6 and results are given in ***Figure 2.10***. The entrapment efficiency was observed to vary from 26 - 62 % when 1 % lamotrigine was added during polymerization of different monomer ratios. UV-spectrum of lamotrigine shows maximum absorbance (λ_{max}) around 306 nm in absolute alcohol ***(Figure 2.10a)*** and that of copolymeric nanoparticles at 235 nm ***(Figure 2.10b)***. The UV-spectrum of lamotrigine loaded copolymeric nanoparticles shows two distinct peaks at 306 and 235 nm corresponding to drug and polymer respectively ***(Figure 2.10c)***. From the calibration plot at 306 nm, entrapment efficiency of lamotrigine in nanoparticles was calculated.

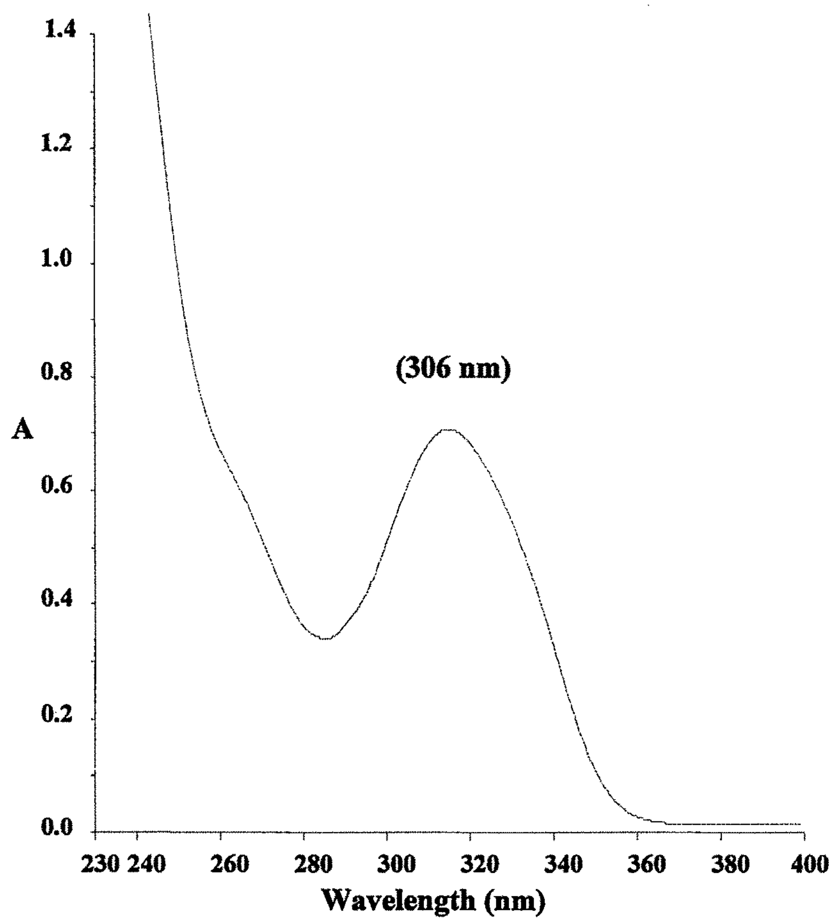

(a)

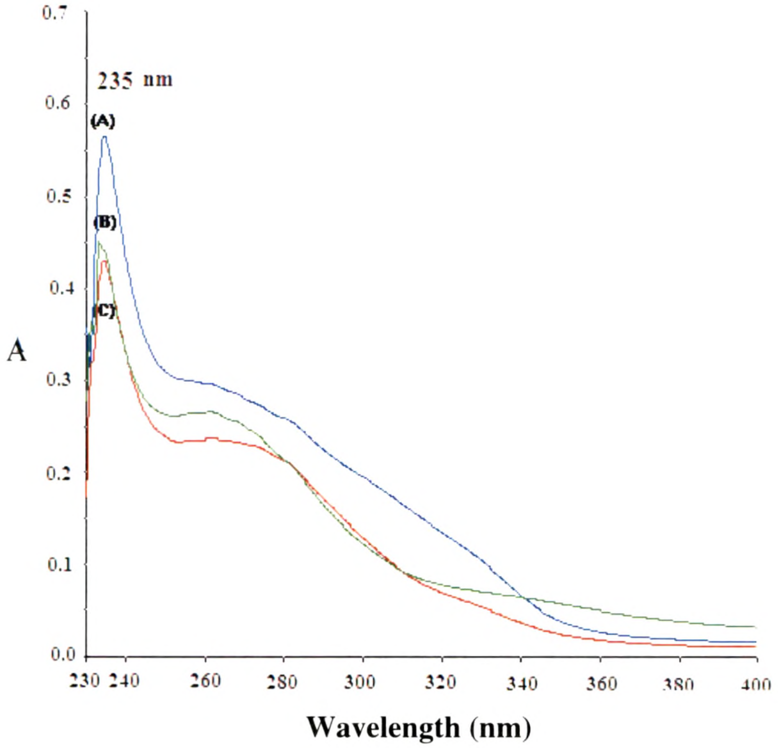

(b)

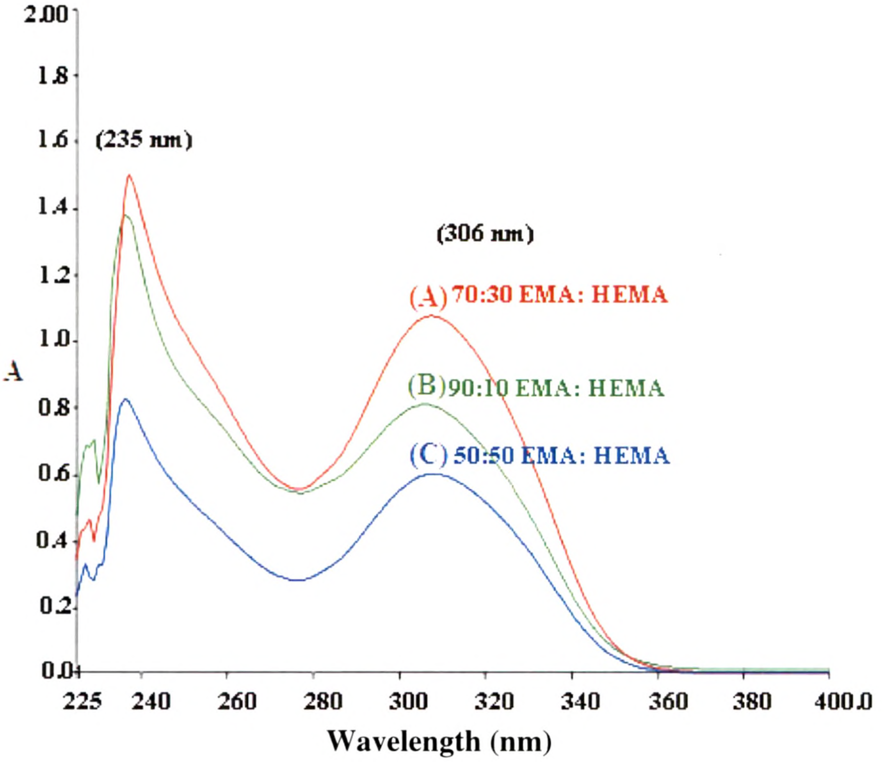

(c)

Figure 2.10 UV spectra of (a) lamotrigine, (b) copolymeric nanoparticles and (c) lamotrigine loaded copolymeric nanoparticles.

Maximum entrapment of lamotrigine was observed for 70:30 EMA: HEMA (A) composition. ***Table 2.5*** shows the entrapment efficiency of lamotrigine loaded copolymeric nanoparticles of different compositions. Variation in encapsulation efficiency (EE) and rate of drug release from copolymeric particles can be attributed to the variation in microstructure of copolymers, which has been correlated to HEMA content[137, 138]. In the present study, percentage encapsulation efficiency was observed to increase up to 30 % of HEMA content in copolymer and thereafter it decreases. This may be because of increased hydrophilicity/polar nature of the copolymer, which discourages lamotrigine to remain inside the copolymeric particle.

Table 2.5 Effect of the monomer ratio on the particle size, % EE of lamotrigine and swelling of nanoparticles.

EMA: HEMA	Particle Size (nm)	PDI	Equilibrium swelling (Q) (%)	Diffusion exponent (n)	r^2	% EE
90: 10	24 ± 0.3	0.11	10.1	0.28	0.93	43 ± 2
80: 20	26 ± 0.7	0.22	12.1	0.29	0.88	54 ± 3
70: 30	25 ± 0.9	0.19	23.6	0.38	0.97	63 ± 3
60: 40	36 ± 0.7	0.16	34.5	0.41	0.97	36 ± 3
50: 50	30 ± 0.6	0.18	41.5	0.45	0.98	27 ± 2

2.3.6 Swelling study

The influence of overall hydrophilicity of copolymers on water transport through them was determined by varying the copolymer hydrophilicity by copolymerization of EMA and HEMA comonomers in different ratios. The results obtained in equilibrium swelling studies performed by equilibrium weight gain method at gastric pH conditions (pH 1.2), for the copolymeric nanoparticles are presented in ***Figure 2.11***. The water uptake was found to be dependant on the copolymer composition. Maximum water uptake observed for 50: 50 EMA: HEMA copolymer composition was 41.5 % and was gradually reduced to 10.4 % with increasing concentration of EMA in copolymer. The reduction in water uptake is due to the increase in hydrophobic character in copolymer. To predict and compare the release behavior of any drug from the polymeric system, it is necessary to fit the data into release kinetic equation.

$$\boxed{\frac{M_t}{M_\infty} = kt^n} \tag{10}$$

Where,

M_t is swelling of nanoparticles with respect to time and

M_∞ is the swelling of nanoparticles at equilibrium.

Values of diffusion exponent (n) calculated from the plot of log M_t / $M\infty$ vs Log t are given in ***Table 2.5.*** It was well known that, values of n near 0.5 indicate Fickion transport process, 0.5 < n < 1.0 indicate anomalous transport, n =1.0 indicates Case – II transport or zero order release and n higher than 1 indicates super case-II transport[141]. In the present work, the observed values of n are in the range of 0.28 to 0.45 indicating more Fickion water transport mechanism.

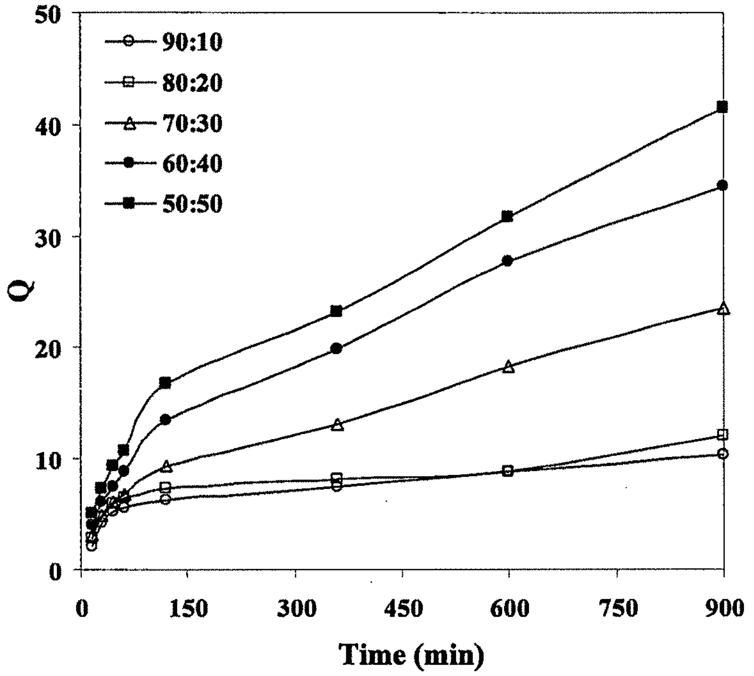

Figure 2.11 Equilibrium swelling study of copolymeric nanoparticles in 0.1 N HCl.

(O) 90:10 (EMA: HEMA), (□) 80:20 (EMA: HEMA),

(Δ) 70:30 (EMA: HEMA), (•) 60:40 (EMA: HEMA), and

(■) 50:50 (EMA: HEMA).

2.3.7 In-vitro release

In vitro dissolution has been recognized as an important element in drug development. Under certain conditions it can be used as a surrogate for the assessment of Bioequivalence. Several theories / kinetics models describe drug dissolution from immediate and modified release dosage forms. There are several models to represent the drug dissolution profiles where f is a function of t (time) related to the amount of drug dissolved from the pharmaceutical dosage system. The quantitative interpretation of the values obtained in the dissolution assay is facilitated by the usage of a generic equation that mathematically translates the dissolution curve in function of some parameters related with the pharmaceutical dosage forms. Some of the most relevant and more commonly used mathematical models describing the dissolution curves are given in ***Table 2.6.***

Table 2.6 Mathematical models used to describe drug dissolution studies.

Models	Mathematical equations
Zero Order	$Q_t = Q_0 + K_0 t$
First Order	$ln\, Q_t = ln\, Q_0 + K_t t$
Second Order	$Q_t / Q_á\, (Q_á - Q_t)\, K_2 t$
Higuchi	$Q_t = K_H\, (t)^{1/2}$
Baker – Lonsdale	$(3/2)\, [1\text{-}(\text{-}1(Q_t / Q_á))^{2/3}] = b\, X \log t - \log a$
Korsmayer – Peppas	$Q_t / Q_á = K_k t^n$
Quadratic	$Q_t = 100(K_1 t^2 + K_2 t)$
Logistic	$Q_t = A / [\, 1 + e^{-K(t-y)}\,]$
Hopfenberg	$Q_t / Q_á = 1 - [1 - k_0 t / C_0 a_0]^n$

The release models with major appliance and best describing drug release phenomena are the Higuchi model, zero order model, first order model and Korsmeyer–Peppas model. We have also tried to correlate the obtained data by above mentioned models. The release of lamotrigine from copolymeric nanoparticles in 0.1M HCl shown in ***Figure 2.12*** shows a two phase release profile.

The first phase shows initial high rate of release for maximum period of 50 min. This is followed by the slow release phase. Total percentage cumulative release upto maximum of 45 % for the batches with 50:50 EMA: HEMA and the minimum of 23 % for 90:10 EMA: HEMA composition for a period of 15 hours shows a sign of controlled and prolonged release of lamotrigine. The initial fast release of drug is the outcome of burst release due to the fast dissolution and quick diffusion of drug particles migrating to the periphery during the formation of the particles by co-acervation or by in-situ polymerization.

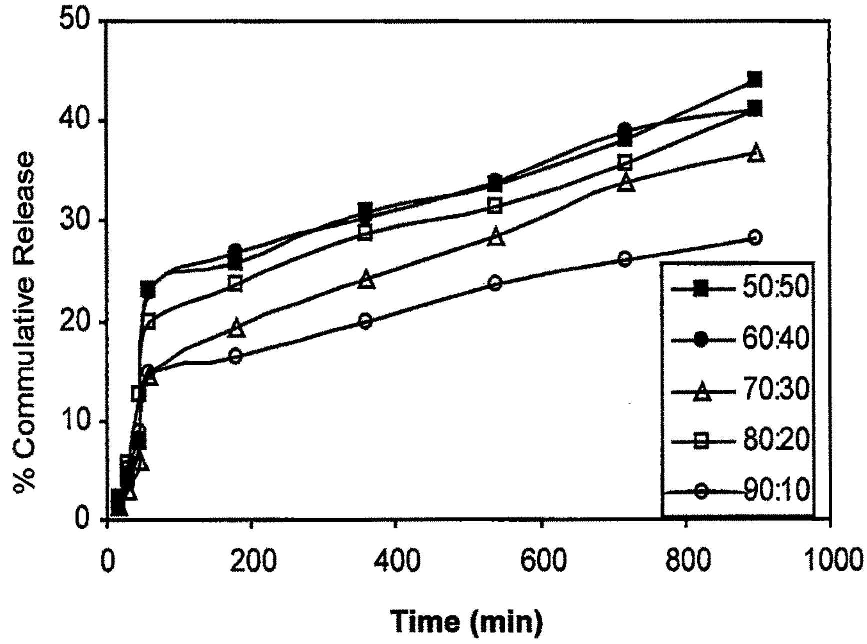

Figure 2.12 Percentage cumulative release pattern of lamotrigine through copolymeric nanoparticles.

(O) 90:10 (EMA: HEMA), (□) 80:20 (EMA: HEMA),

(Δ) 70:30 (EMA: HEMA), (•) 60:40 (EMA: HEMA), and

(■) 50:50 (EMA: HEMA).

The extent of drug accumulation at the boundary depends on many parameters such as, differential solubility of drug and the polymer in the common solvent in case of co-acervation while, it may be the difference in the rate of precipitation of the drug and the rate of polymerization of the monomer during in-situ polymerization process. In addition, a drug like lamotrigine having low partition coefficient at acidic pH diffuses faster in the hydrophilic polymer matrix than in a hydrophobic polymer matrix. A similar observation is made in the present case, where copolymers with higher hydrophobic character shows lower burst (~15 %) than those with low hydrophobicity.

Kinetics of the first phase release can be obtained by plotting the cumulative percentage drug release vs time for Zero order, log % release vs t for First order, % release vs $t^{1/2}$ for Huguchi model and fractional release M_t/M_∞ vs t for Peppas model.

Table 2.7 gives calculated kinetic constants and correlation co-efficients (r^2) for these methods and models.

Table 2.7 Kinetic parameters of the first phase release of drug.

EMA :HEMA	Zero		First		Higuchi		Peppas	
	k_o	r^2	k_1	r^2	k_h	r^2	n	r^2
90:10	0.23	0.99	0.03	0.98	2.43	0.98	1.37	1.00
80: 20	0.36	0.97	0.03	0.91	3.7	0.94	1.66	0.99
70: 30	0.15	0.97	0.02	1.00	1.57	0.94	1.29	0.99
60: 40	0.19	1.0	0.02	1.00	2.00	0.92	1.22	0.99
50: 50	0.23	0.96	0.03	0.98	2.38	0.99	1.71	1.00

The kinetic constant of release (k) was found to be independent of the composition of the copolymer. This may be due to the fact that the maximum release during this phase is due to fast dissolution of drug molecules adsorbed at the surface and diffusion process has little to do in this phase. It was interesting to note that all copolymers showed r^2 nearer to unity with Peppas model, indicating the role of polymer relaxation in the nanoparticle surface in dislodging the drug molecule and release as discussed by Peppas[140].

The second phase of release profile is almost linear in all the batches and the calculated parameters are given in ***Table 2.8.*** The mechanism of release in this phase from a matrix is generally by diffusion of drug through matrix or by polymer erosion/ degradation in the release media[141]. The kinetics of drug release in a matrix by diffusion is explained first time by Higuchi[142, 143] and the proposed mathematical model relates the cumulative percentage drug release proportional to the square root of time ($t^{1/2}$). Kinetics of the second phase release profile studied shows r^2 relatively nearer to unity with respect to zero order kinetic model. This pattern of release is generally due to polymer degradation in the matrix particularly by surface erosion. However, it is quite difficult to confirm the mechanism with the existing experimental observations as the combination of several other processes including high swelling behavior could also show zero order like kinetics.

Table 2.8 Kinetic parameters of the second phase release of drug.

EMA :HEMA	Zero k_o	Zero r^2	First k_1	First r^2	Higuchi k_h	Higuchi r^2	Peppas n	Peppas r^2
90: 10	0.02	0.99	0.0003	0.98	0.62	0.98	0.24	0.93
80: 20	0.02	0.99	0.0004	0.98	0.91	0.97	0.25	0.95
70: 30	0.03	0.99	0.0005	0.98	1.01	0.99	0.34	0.98
60: 40	0.02	0.99	0.0003	0.96	0.90	0.98	0.22	0.96
50: 50	0.02	0.99	0.0003	0.99	0.83	0.95	0.22	0.91

Overall in a limited sense we can say First phase of drug release is well explained by Peppas model whereas second phase of drug release shows better agreements with zero order model.

2.3.8 Stability studies

The stability studies were carried out according to USP/ICH guidlines[144, 145]. The study was carried out upto 3 months storage time. The lyophilized nanoparticles were stored at defined conditions and retained drug was determined at specific time intervals. Similarly, particle size of the synthesized latex was determined at defined condition for a specific time interval. It was observed from the results in ***Table 2.9*** that, up to 70:30 EMA: HEMA composition no agglomeration at 2-8 °C is observed & for 60:40 and 50:50 EMA: HEMA composition, some agglomeration at 2-8 °C is observed. At room temperature (30 ± 2 °C), extent of agglomeration is relatively higher and observed to be dependant on HEMA content in copolymer.

Figure 2.13 A and B show the percentage drug retained with time in the copolymeric nanoparticles at 2-8 °C and 30 ± 2 °C respectively. It was observed that 5-10 % loss due to leaching of drug takes place at lower temperature for various compositions of EMA: HEMA copolymer after 3 months storage. At room temperature (30 ± 2°C) the loss due to leaching of drug was 5-22 % for these copolymer compositions. Polymeric nanoparticles showed better stability at lower temperature.

Table 2.9 Effect of temperature & storage time on stability of nanoparticles.

EMA : HEMA	Particle size (nm)							
	Storage time at 2-8 ^{O}C in months				Storage time at 30 ± 2 ^{O}C in months			
	0	**1**	**2**	**3**	**0**	**1**	**2**	**3**
90: 10	24 ± 3	26 ± 3	27 ± 4	30 ± 2	24 ± 3	27 ± 1	32 ± 2	37± 2
80: 20	26 ± 2	28 ± 3	29 ± 2	31 ± 2	26 ± 2	33 ± 4	40 ± 3	42 ± 2
70: 30	25 ± 2	28 ± 2	30 ± 2	32 ± 3	25 ± 2	38 ± 5	42 ± 3	49 ± 5
60: 40	35 ± 2	46 ± 5	52 ± 5	52 ± 5	36 ± 2	50 ± 3	54 ± 5	62 ± 4
50: 50	30 ± 3	39 ± 5	58 ± 4	60 ± 4	30 ± 3	67 ± 1	70 ± 4	76 ± 5

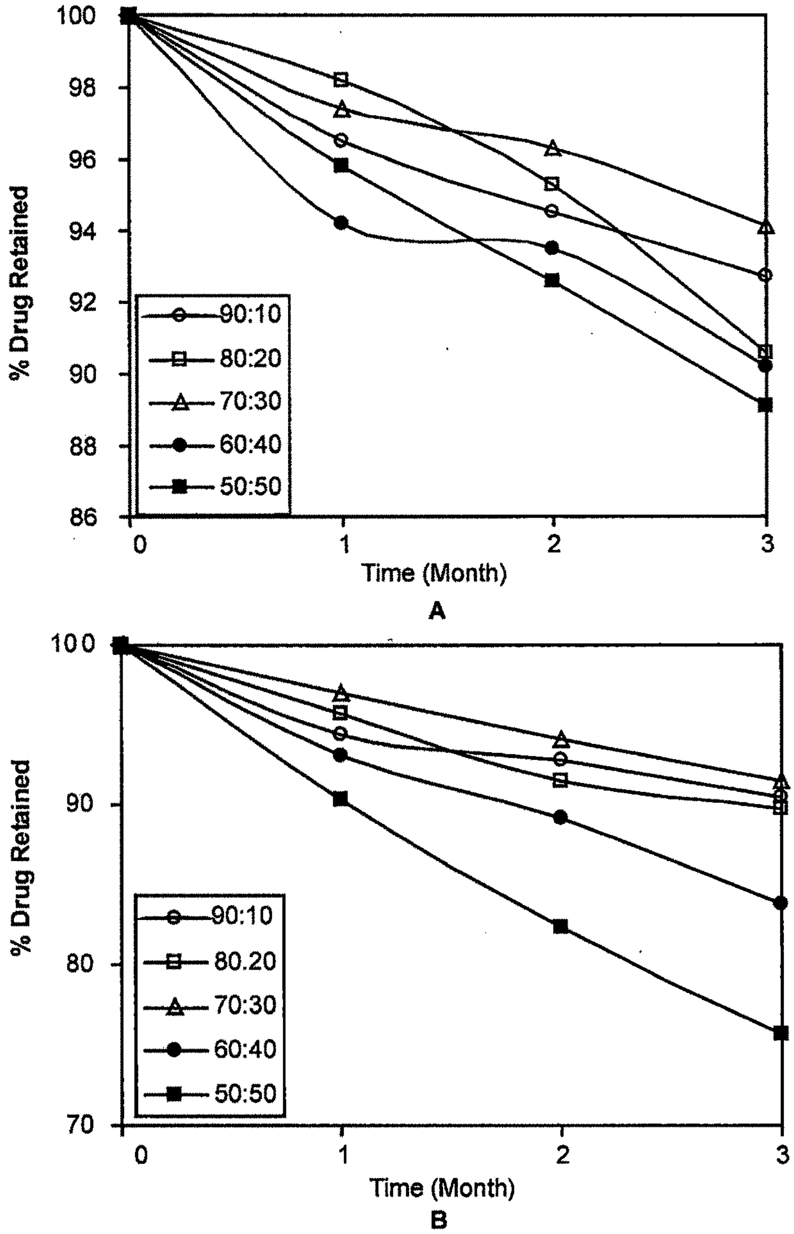

Figure 2.13 **Percentage drug retained (A) at 2-8 °C and (B) at 30 °C from copolymeric nanoparticles with respect to time. (O) 90:10 (EMA: HEMA), (□) 80:20 (EMA: HEMA), (Δ) 70:30 (EMA: HEMA), (•) 60:40 (EMA: HEMA), and (■) 50:50 (EMA: HEMA).**

2.4 Conclusion

Copolymeric nanolatex of poly (EMA-co-HEMA) was prepared through a microemulsion polymerization technique. Monomer reactivity ratios determined by Fineman-Ross, Inverted Fineman-Ross, Kelan-Tudos, linear least square methods and Tidwell-Mortimer nonlinear least square methods, showed good correlation between them. It was observed that the monomer pair under investigation has a tendency to form random copolymer. TEM and DLS analysis of nanolatex confirmed the formation of well defined reasonably well mono-dispersed particles of approximetly 30 ± 5 nm size with nearly spherical morphology. The addition of a model drug lamotrigine, to polymeric nanoparticles synthesized through microemulsion polymerization proved to be successful with a 26-62 % drug entrapment with respect to copolymer compositions. The incorporation of lamotrigine did not appear to interfere significantly in the physicochemical properties of the polymer such as structure, particle size and morphology. IR and ^{1}H NMR analysis confirmed the copolymer formation. UV analysis indicates the molecular level dispersion of drug in polymeric matrix. TEM and DLS analysis of nanolatex confirmed the formation of well defined reasonably well mono-dispersed particles with spherical morphology. As the HEMA content increases in copolymer, increase in leakage of lamotrigine with time was observed at both the temperatures. Release profile of lamotrigine from copolymeric nanoparticles shows initial burst effect followed by continuous slow release for a period of 15 hours indicating a sign of controlled release of lamotrigine from nanoparticles.

2.5 References

1. Zhang L.D., Mou J.M., *'Nanomaterials and Nanostructure'*., Science Press, Beijing, 2001.
2. Decher G., *Science.,* 1997, **277**, 1232.
3. Zhang Z.Y., Yin Y.D., Gates B., Xia Y.N., *Adv. Mater.,* 2000, **12,** 206.
4. Crooks R.M., Zhao M, Sun L.J., *Am. Chem. Soc.,* 1998, **120,** 4877.
5. Smith A.P., Spontak R.J., Ade H., Smith S.D., Koch C.C. *Adv. Mater.* 1999, **11**, 1227.
6. Jaykrishshnan A., Shah D.O., *J. Polym. Sci. Polym. Lett. Ed.,* 1984, **22,** 31.
7. Hoar T.P., Schulman J.H., *Nature.,* 1943, **152**, 102.
8. Schulman J.H., Stoeckenius W., Price L.M., *J. Phys. Chem.,* 1959, **63,** 1677.
9. Stoffer J.O., Bone T., *J. Disper.Sci.Technol.,* 1980, **1**, 37.
10. Stoffer J.O., Bone T., *J. Polym. Sci.*, 1980, **18,** 2641.
11. Atik S.S., Thomas J.K., *J. Am. Chem. Soc.*, 1981, **103,** 4279.
12. Johnson P.I., Gulari E., *J. Polym. Sci. Polym. Chem. Ed.,* 1984, **22,** 3967
13. Candau F., Leong Y.S., Fitch R.M., *J. Polym. Sci. Part A: Polym. Chem.*, 1985, **23**, 193.
14. Candau F., Zekhnini Z., Durand J.P., *J. Colloid Interface Sci.,* 1986, **114,** 394.
15. Candau F., *J. Chem. Phys. Phys. Chem. Biol.,* 1987, **84,** 1095.
16. Candau F., Zekhnini Z., Durand J.P., *Prog. Colloid Polym. Sci.,* 1987, **73,** 33.
17. Guo J.S., El-Aasser M.S., Vanderhoff J.W., *J. Polym. Sci. Part A: Polym. Chem. Ed.* 1989, **27,** 691.
18. Puig J.E., Corona-Gavlen. S., Maldonado A., Schulz P. *J. Colloid Interface Sci.,* 1990, **137**, 308.
19. Gan L.M., Chew C.H., Lye I., Imae, T., *Polym. Bull.,* 1991, **25,** 193.
20. Gan L.M., Chew C.H., Lye I., Ma L., Li G.Z., *Polymer.,* 1993, **34,** 3860.
21. Gan L.M., Lian N., Chew C.H., Li G.Z., *Langmuir.,* 1994, **10,** 2197.
22. Roy S., Devi S., *J. Appl. Polym. Sci.*, 1996, **62,** 1509
23. Roy S., Devi S., *Polymer*., 1997, **38,** 3325.
24. Xu X., Ge X., Zhang Z., Zhang M., Zuo M., Niu A., *Polym. Int.,* 1998, **47,** 393.
25. Pokhrial N.K., Devi. S., *Eur. Polym. J.,* 2000, **36**, 333.

26. Pokhrial N.K., Sanghvi P.G., Hassan P.A., Devi. S., *Eur. Polym. J.,* 2001, **37**, 1695.
27. Arias J.L., Gallardo V., Gomez-Lopera S.A., Plaza R.C., Delgado A.V., *J. Control. Release.,* 2001, **77**, 309.
28. Vauthier C., Dubernet C., Chauvierre C., Brigger I., Couvreur P., *J. Control. Release.,* 2003, **93,** 151.
29. Sullivan C.O., Birkinshaw C., *Biomaterials.,* 2004**, 25**, 4375.
30. Ramana Reddy G.V., Magesh, C., Sriram R., *Desgn. Monomer Polym.,* 2005**, 8**, 75.
31. Sarciaux J.M., Acer I., Sado P.A., *Int. Pharm. Sci.,* 1995, **120,** 127.
32. Gangopadhyay R., De A., *Chem. Mater.,* 2000, **12**, 608.
33. Antonietti M., Nestl T., *Macromol. Rapid Comm.,* 1994, **15,** 111.
34. Zhang C., Wang Q., Xia H., Qiu G., *Eur. Polym. J.,* 2002, **38,** 1769.
35. Xu P., Zhong W., Wang H., Tong R., Du Q., *Colloid Polym. Sci.,* 2004, **282**, 1409.
36. Wen S., Yin X., Stevenson W.T.K., *J. Appl. Polym. Sci.* 1991, **43,** 205.
37. Gallar do J., Roman J.S., *Polymer.*, 1993, **34**, 567.
38. Barannon-Peppas L., Peppas N.A., *Biomaterials.*, 1990, **11**, 635.
39. Montheard J.P., Chatzopoulos M., Chappard D., *J. Macro. Sci.-Rev. Macro. Chem. Phys.,*1992, *C*32, 1.
40. Singh J., Agrawal K.K., *J. Macro. Sci.-Rev. Macro. Chem. Phys.* 1992, C32, 521.
41. Mark H.F., Bikales N.M., Overberger C.G., Menges G., *Encyclopedia Polym. Sci. and Eng.,* 1985, **1,** 234.
42. Martinez G., Sanchez Chaves M., Madruga E.L., Ferrandez-Monreal C., *Polymer.*, 2000, **41**, 6021.
43. Jeyanthi R., Rao P.K., *Biomaterials.*, 1990, **11**, 238.
44. Ratner B.D., *J. Biomed. Mater. Res.*, 1993, **27**, 283.
45. Williams D.F., *Concise Encyclopedia of Medical and Dental Materials,* Pergamon Press, Oxford, 1990.
46. Beers K.L., Boo S., Gaynor S.G., Matyjaszewski K., *Macromolecules.*, 1999, **32**, 5772.
47. Coca S., Jasieczek C.B., Beers K.L., Matyjaszewski K., *J. Poly. Sci. Part A: Poly. Chem.,* 1998, **36**, 1417.

48. Robinson K.L., Khan M.A., Paz Benez M.V., Wang X.S., Armes S.P., *Macromolecules.*, 2002, **34**, 3155.
49. Tiemblo P., Laguna M.F., Garcia F., Garcia J.M., Riande E., Guzman J., *Macromolecules.*, 2004, **37**, 4156.
50. Hill D.J.T., O'Donnell J.H., Pomery P.J., *Polym. Gels Netw.*, 1995, **3**, 85.
51. Moss N.G., Pomery P.J., Whittaker A.K., *Polymer.,* 1999, **41**, 1287.
52. Peppas N.A., Moynihan H.J., *In: Hydrogels in medicine and pharmacy, II.* Peppas N.A., (Eds.), Boca Raton, FL: CRC Press, 1987, 49.
53. Tighe B.J., *In: Hydrogels in medicine and pharmacy, III.,* Peppas N.A. (Eds.), Boca Raton, FL: CRC Press, 1987, 53.
54. Martin A., Swarbrick J., Cammarata A., *Physical pharmacy*, Philadelphia, PA: Lea and Febiger., 1983, 579.
55. Shah S.S., Pal A., Rajyaguru T., Murthy R.S.R. Devi. S., *J. Appl. Polym. Sci.,* 2008, **107,** 3221.
56. Liu D., Ichikawa H., Cui F., Fukumori Y., *Int. J. Pharm.,* 2006, **307,** 300.
57. Yan X., Gemeinhart R.A., *J. Control Release.,* 2005, **106,** 198.
58. Hill D.J.T., Moss N.G., Pomery P.J., Whittaker A.K., *Polymer.,* 2000, **41,** 1287.
59. Barson C.A., Rizvi M.S., *Eur. Polym. J.*, 1970, **6**, 241.
60. Barson C.A., Turner M.J., *Eur. Polym. J.*, 1973, **9**, 789.
61. Barson C.A., Turner M.J., *Eur. Polym. J.*, 1974, **10**, 917.
62. Barson C.A., Turner M.J., *Europ. Polym. J.*, 1974, **10**, 1053.
63. Verma I.K., Patnaik S., *Eur. Polym. J.,* 1976, **12,** 259.
64. Garcia M.F., Torrado M.F., Martinez G.,Sanchez-Chaves M., Madruga. E.L., *Polymer.,* 2000, **41**, 8001.
65. Ito K., Uchida K., Kitano T., Yamada E., Mutsumoto T., *Polym J.,* 1985, **17**, 761.
66. Gan L.M., Lee K.C., Chew C.H., Ng S.C., Gan L.H., *Macromolecules.,* 1994, **27,** 6335.
67. Xu X., Chew C.H., Siow K.S., Wong M.K., Gan L.M., *Langmuir.,* 1999, **15,** 8067.
68. Sanghvi P.G., Pokhriyal N., Devi S., *J. Appl. Polym. Sci.,* 2002, **84**, 1832.
69. Polic A.L., Duever T.A. Penlidis A., *J. Polym. Sci.: Part A.,* 1998, **36,** 813.
70. Abdollahi M., Sharifpour M., *Polymer.,* 2007, **48,** 25.

71. Aguilar M.R., Gallardo A., Fernandez M.M., Román J.S., *Macromolecules.*, 2002, **35**, 2036.
72. Belleney J., Hélary G., Migonney V., *Eur. Polym. J.*, 2002, **38**, 439.
73. Bernhardt S., Glöckner P., Ritter H., *Polym. Bull.*, 2001, **46,** 153.
74. Bhawal S., Devi S., *J. Appl. Polym. Sci.*, 2002, **86**, 2802.
75. Bhawal. S., Sanghvi P.G., Devi S., *Eur. Polym. J.*, 2002, **39**, 389.
76. Brar A.S., Dutta K., *Macromol. Chem. Phy.*, 1998, **199,** 2005.
77. Brar A.S., Hekmatyar S.K., *J. Appl. Polym. Sci.*, 1999, **74,** 3026.
78. Brar A.S., Yadav A., *Polym J.*, 2003, **35,** 37.
79. Brar A.S., Kaur. M., *Eur. Polym. J.*, 2003, **39,** 705.
80. Brar A.S., Hooda S., Goyal A., *J. Mol. Structure.*, 2007, **828**, 25.
81. Buback M., Wittkowski L., *Macromol. Chem. Phy.*, 2000, **201,** 419.
82. Camail M., Essaoudi H., Gedoux B., *Eur. Polym. J.*, 1998, **34**, 1007.
83. Catalgil-Giz H., Giz A., Alb A. M., *Macromolecules.*, 2002, **35,** 6557.
84. Chambard G., Klumperman B., German A.L., *Polymer.*, 1999, **40,** 4459.
85. Coskun M, Ilter Z., *J. Polym. Sci., Part A: Polym. Chem.*, 2002, **40**, 1184.
86. Coskun M.F., Demirelli K., Güzel D., Coskun M., *J. Polym. Sci., Part A: Polym. Chem.*, 2002, **40**, 650.
87. Czerwinski W.K. *Polymer.* 1998, **39**, 183 (a) and Czerwinski W. K., *Polymer.*, 1998, **39,**189.
88. De P., Sathyanarayana D.N., *Macromol. Chem. Phy.*, 2002, **203**, 2218.
89. De P., Sathyanarayana D.N., *J. Polym. Sci. Part A: Polym. Chem.*, 2002, **40,** 9.
90. De P, Sathyanarayana D.N., *J. Polym. Sci. Part A: Polym. Chem.*, 2002, **40,** 564.
91. Demirelli K., Kaya I., Coskun M., *Polymer.*, 2001, **42,** 5181.
92. Ydens S., Degee P., Haddleton D.M., Dubois P., *Eur. Polym. J., 2005*, **41,** 2255.
93. Erbil C., Ozdemir S., Uyanik N., *Polymer.*, 2000, **41,** 1391.
94. Erol I., Soykan C., *J. Macromol. Sci. Pure & Appl. Chem.*, 2002, **39**, 953.
95. Fernández-García M., Fernández-sanz M., Madruga E.L., *J. Polym. Sci. Part A: Polym. Chem.*, 2000, **38,** 60.
96. Fernández-García M., Sánchez-Chaves M., Martínez G., Madruga E.L., *Acta Polymerica.*, 1999, **50**, 408.

97. Galimberti M., Piemontesi F., Fusco O., *Macromolecules.,* 1998, **31,** 3409.

98. Galimberti M., Piemontesi F., Mascellani N., *Macromolecules.,* 1999, **32,** 7968.

99. Habibi A., Vasheghani-Farahani E., Semsarzadeh M. A., Sadaghiani K., *Macromol. Theo. Simul.,* 2003, **12,** 184.

100. Haddleton D.M., Crossman M.C., Hunt K.H., *Macromolecules.,* 1997, **30,** 3992.

101. Hakim M., Verhoeven V., Mcmanus N.T., Dube M.A., Penlidis A., *J. Appl. Polym. Sci.,* 2000, **77,** 602.

102. Hill D.J.T., Lang A.P., O'Donnell J.H., O'Sullivan P.W., *J. Appl. Polym. Sci.,* 1989, **25,** 911.

103. Ito H., Dalby C., Pomerantz A., *Macromolecules.,* 2000, **33**, 5080.

104. Kaim A., *J. Polym. Sci. Part A: Polym. Chem.,* 2000, **38,** 846.

105. Kaim A., *Macromol. Theo. Simul.,* 1998. **7,** 97.

106. Kaim A., Oracz P., *Polymer.,* 1999, **40**, 6925.

107. Kaim A., Oracz P., *Polymer.,* 1998, **39**, 3901.

108. Kucharski M., Lubczak R., *J. Appl. Polym. Sci.,* 1997, **64,** 1259.

109. Manders B.G., Smulders W., Aerdts A.M., Vanherk A.M., *Macromolecules.,* 1997, **30**, 322.

110. Martineza G., Sanchez-Chavesa M., Madruga E.L, Monreal F., *Polymer.,* 2000, **41,** 6021.

111. McManus N.T., Penlidis A., Rempel G.L., *Dev. Chem. Eng. Miner. Proc.,* 1998, **6**, 153.

112. Mcmanus N.T., Kim J.D., Penlidis A., *Polym. Bull.,* 1998, **41**, 661.

113. Mcmanus N.T., Penlidis A, Dube M.A., *Polymer.,* 2002, **43,** 1607.

114. Monett D., Méndez J.A., Abraham G.A., M*acromol. Theo. Simul.,* 2002, **11**, 525.

115. Palmer D.E., Mcmanus N.T., Penlidis A., *J. Polym. Sci, Part A: Polym. Chem.,* 2001, **39,** 1753.

116. Palmer D.E., Mcmanus N.T., Penlidis A., *J. Polym. Sc., Part A: Polym. Chem.,* 2000, **38,** 1981.

117. Rainaldi I., Cristallini C., Ciardelli G., Giusti P., *Macromol. Chem. Phy.,* 2000, **201**, 2424.

118. Roos S.G., Mueller A.H.E., Matyjaszewski K., *Macromolecules.,* 1999, **32,** 8331.
119. Ryttel A., *J. Appl. Polym. Sci.,* 1999, **74,** 2924.
120. Sanghvi P.G., Patel A.C., Gopalkrishnan K.S., Devi S., *Eur. Polym. J.,* 2000, **36,** 2275.
121. Scorah M.J., Hua H., Dube M.A., *J. Appl. Polym. Sci.,* 2001, **82,** 1238.
122. Senthilkumar U., Balaji R., Nanjundan S., *J. Appl. Polym. Sci.,* 2001, **81,** 96.
123. Stergiou G., Dousikos P., Pitsikalis M., *Eur. Polym. J.,* 2002, **38,** 1963.
124. Thamizharasi S., Gnanasundaram P., Reddy B.S.R., *Eur. Polym. J.,* 1997, **33,** 1457.
125. Thamizharasi S., Gnanasundaram P., Reddy B.S.R., *J. Appl. Polym. Sci.,* 1997, **65,** 1285.
126. Thamizharasi S., Gnanasundaram P., Balasubramanian S., *J. Macromol. Sci. Pure & Appl. Chem.,* 1999, **36,** 1949.
127. Thamizharasi S., Srinivas G., Sulochana N., Reddy B.S.R., *J. Appl. Polym. Sci.,* 1999, **73,** 1153.
128. Van Den Brink M., Smulders W., Van Herk A.M., German A.L., *J. Polym. Sci. Part A: Polym. Chem.,* 1999, **37,** 3804.
129. Vijayanand P.S., Penlidis A., Nanjundan S., *J. Macromol. Sci. Pure Appl. Chem.,* 2003, **40,** 125.
130. Vijayanand P.S., Penlidis A., Radhakrishnan S., Nanjundan S., *J. Macromol. Sci. Pure Appl. Chem.,* 2002, **39,** 591.
131. Zaldivar C., del Sol O., Iglesias G.D., *Polymer.,* 1997, **39,** 1997.
132. Zhao Y., Li H., Liu P., *J. Appl. Polym. Sci.,* 2002, **83,** 3007.
133. Ziaee F., Nekoomanesh M., *Polymer.,* 1997, **39,** 203.
134. Fineman M., Ross S.D., *J. Polym. Sci.,* 1950, **5,** 259.
135. Kelen T, Tudos F., *J. Macromol. Sci. Chem.,* 1975, **9,** 1.
136. Tidwell P.W., Mortimer G.A., *J. Polym. Sci., Part A: Polym. Chem.,* 1965, **3,** 369.
137. Sanghavi P.G., Devi S., *Int. J. Poly. Mater.,* 2005, **54,** 293.
138. Schmuhl N., Brault, D., Cheung, H. M., *Langmuir.,* 1998, **14,** 757.
139. Costa P., Lobo J.M.S., *Eur. J. Pharma. Sci.,* 2001,13,123.
140. Peppas N.A., *Acta. Helv.,* 1985, **60,** 110.
141. Zhou S.B., Deng X.M., Li X.H., *J. Control. Release.,* 2005, **75,** 27.

142. Higuchi T., *J. Pharm. Sci.,* 1961, **50**, 874.

143. Higuchi T., *Pharm. Tech.*, 1963, **10**, 24.

144. http:// www.fda.gov/cder/guidance/index.htm

145. Daoud-Mahammed S., Couvreur P., Gref R., *Int. J. Pharm.*, 2007, **332,** 185, 36.